Fuel from Waste - Catalytic degradation of plastic waste to liquid fuels

Agnieszka Ćwik

Thesis to obtain the Master of Science Degree in

Energy Engineering and Management

Examination Committee

Chairperson: Prof. José Alberto Caiado Falcão de Campos

Supervisors: Professor Maria Amelia Lemos , Prof. Teresa Grzybek

Member of the Committee: Prof. João Bordado, Prof. Maria de Fatima Montemor

February, 2014

Fuel from Waste - Catalytic degradation of plastic waste to liquid fuels

Ćwik Agnieszka

Supervisors: Professor Maria Amelia Nortadas Duarte de Almeida Lemos

Professor Francisco Manuel da Silva Lemos

Professor Teresa Grzybek

February, 2014

Acknowledgments

I would like to thank to Professor Amelia Lemos and Professor Francisco Lemos for the great contributions to knowledge and guidance important for the preparation of this work. I really appreciate their help, support and attention I had during this research work.

I would also like to acknowledge Professor Teresa Grzybek for her help, patience and motivation, despite of the distance.

Therefore I would like to thank all people for encouragement and support during my research work, special thanks to David and Andre. Also, I want to express my gratitude to other 'Clean Coal' Students for the motivation to finish this thesis.

At the end I would also mentioned my parents, thank them for their support and encouragement in each step of working on this thesis.

To all of them, I would like to say my deepest thanks.

Acknowledgments

This thesis is based on work conducted within the KIC InnoEnergy Master School, in the MSc programme Clean Coal Technologies. This programme is supported financially by the KIC InnoEnergy. The author also received financial support from KIC InnoEnergy, which is gratefully acknowledged.

KIC InnoEnergy is a company supported by the European Institute of Innovation and Technology (EIT), and has the mission of delivering commercial products and services, new businesses, innovators and entrepreneurs in the field of sustainable energy through the integration of higher education, research, entrepreneurs and business companies. Shareholders in KIC InnoEnergy are leading industries, research centres, universities and business schools from across Europe.

www.kic-innoenergy.com

The MSc programme Clean Coal Technologies is a collaboration of:

AGH University of Science and Technology, Kraków, Poland,

SUT Silesian University of Technology, Gliwice, Poland

IST Instituto Superior Tecnico, Lisbon, Portugal

Abstract

In this work, thermal and catalytic degradation of polypropylene with, and without additives are analyzed using thermogravimetry (TG) and differential scanning calorimetry (DSC) methods under a nitrogen atmosphere.

During the first part of the experiments the thermal pyrolysis of both types of polypropylene was carried out using non-isothermal conditions, with different heating rates.

In the second part of the experiments the catalytic pyrolysis of the same polypropylenes was analyzed using 3 groups of catalysts:

- zeolites, namely HZSM-5, HY, Beta and H-Beta
- vermiculites with supported metals, namely silver, zirconium, alumina and copper,
- montmorillonites, including Mt_6OAlCu, K10 + Cu^{2+} and K10 Al Ag^{+}.

From the results obtained, the zeolites were the most effective catalysts for the reduction of the temperature of degradation. Montmorillonites were also somewhat effective for the polyolefin pyrolysis. In contrast, vermiculites, particularly those with metal supported, showed an apparent inactivity proving to be ineffective in the reduction of the temperature degradation.

The simultaneous use of the signals from the TG and DSC helped to develop a kinetic model that is able to describe runs performed for the thermal degradation of both types of polypropylene. Fitting this model to the experimental results allowed the estimation of several kinetic and thermodynamics parameters associated with the degradation of polypropylene.

KEYWORDS: Polypropylene, kinetic modelling, thermal and catalytic degradation, differential scanning calorimetry (DSC), thermogravimetry (TG), plastics, pyrolysis.

Resumo

Neste trabalho, são analisadas a degradação térmica e catalítica de polipropileno com e sem aditivos utilizando a técnica de termogravimetria (TG) e o método de varrimento diferencial de calorimetria (DSC), numa atmosfera de azoto.

Durante a primeira parte de experimentações foi efectuada a pirólise térmica de ambos os tipos de polipropileno, em condições isotérmicas, com taxas de aquecimento diferentes.

Na segunda parte do trabalho, procedeu-se à análise da pirólise catalítica do polipropileno, usando 3 grupos de catalisadores:

- Zeólitos, nomeadamente HZSM-5, HY, Beta e Beta-H;

- Vermiculites com metais de suporte, tais como a prata, o zircónio, alumina e cobre;

- Montmorillonites, incluindo Mt6OAlCu, $K10^{+}$ $Cu2^{+}$ e K10 Al Ag^{+} .

A partir dos resultados obtidos, os Zeólitos foram o catalisador mais eficaz para a redução da temperatura de degradação. As Montmorillonites também foram precisos para a pirólise de poliolefinas. Por outro lado, as Vermiculites, particularmente aqueles com metal suportado, mostraram uma aparente inatividade e pouca eficácia na redução da degradação da temperatura.

O uso simultâneo dos sinais do TG e DSC ajudou no desenvolvimento de um modelo cinético capaz de descrever a degradação térmica de ambos os tipos de polipropileno. Este modelo, depois de aperfeiçoado, foi combinado com os resultados experimentais e capaz de estimar vários parâmetros termodinâmicos e da cinética da reacção.

NOMENCLATURE

PP – Polypropylene

PE – Polyethylene

PVC – Polyvinylchloride

PS – Polystyrene

PET - Polyethylene Terephthalate

MSW - Municipal Solid Waste

DSC - Differential Scanning Calorimetry

TA - Thermal Analysis

TG – Thermogravimetry

TGA - Thermogravimetric Analysis

DFT - Density Functional Theory

DTG - Derivative thermogravimetry

S_{ext} - External surface area

N - Number of C-C bonds per unit mass

n - Carbon atoms

k(T) - Corresponding temperature-dependent rate constant

T_{ref} - Reference temperature chosen within the range of significant weight loss (573 K in this case)

E_a - Apparent activation energy

k_{ref} - Kinetic constant at the reference temperature (Tref)

m - Weight of the sample

C_p - Average heat capacity

ΔH_{C-C} - Average C-C bond enthalpy

ΔH_{vap} - Average vaporization enthalpy per unit mass

k - Kinetic constant rate

n - Order of the reaction in respect to the polymer

m_0 - Initial mass

X - Ratio between the solid weight loss at a given time and the initial solid weigh

X_{max} - Maximum conversion that can be achieved

T_{degrad}. - Degradation temperature

k_0 - Pre-exponential factor

R - Universal gas constant (0.008314 kJ mol-1K-1).

ΔH - Reaction enthalpy,

VAP ΔH - Vaporization enthalpy

Cp - Heat capacity

ΔH_f - Standard molar enthalpy of formation

General Index

INDEX OF FIGURES

INDEX OF TABLES

CHAPTER 1. Introduction

1.1 Motivation and Objectives

Polypropylenes and polyethylenes, two of the major polyolefins in the market of plastics, are some of the main chemical substances produced worldwide. Production of polyethylene and polypropylene accounts for about 50% of all manufactured synthetic polymers. With the threat of ending fuel resources, it is important to find other alternative sources of energy and to provide a better use for the hydrocarbons obtained from oil. Recycling of polyolefins can be part of the possible solutions.

In this work, there are two major objectives. The first one is the study of the pyrolysis of polypropylene, as a good alternative for management of these plastic wastes. The second one is the study of the influence of three types of catalysts on the plastic's degradation.

In the first part of this work possible catalysts suitable to improve degradation of plastics are studying: lowering the pyrolysis temperature and resulting in better quality products.

The second part of the research is made based on influence of catalysts on polypropylene degradation process.

Both thermal and catalytic degradation of waste polyolefins leads to hydrocarbons production, that can be used as blending component in fuels.

A kinetic model is also be used to allow a more detailed picture of the evolution of the reaction, based on TG and DSC scans.

1.2 Polymers

Polymers are natural or synthetic molecules that are composed of a large number of smaller moities, monomers, which have reacted to form a long chain. The most basic polymers are made from the same monomers – the name of this substance is made by adding prefix ‘Poly’ to the name of the monomer. For example, the polymer obtained from propylene is poly(propylene), in common usage the brackets are omitted.

In today’s world most of the polymers used are synthetic. They are produced by reactions of polymerization involving the formation of chemical bonds between the monomer molecules to give rise a long-chain polymer. There is also the possibility to synthesized polymers from different monomers. Products of this reactions are called copolymers, with the starting molecules referred to as comonomers [1,2].

1.2.1 Polymers Classification

Polymers are usually classified by two mayor criteria: according to their thermal behavior and to the polymerization mechanism. From the polymer recycling point of view, this classification is important because the most suitable method of degradation for a given polymer is related to the properties of the molecule.

In common usage, the term ‘plastic’ is considered equivalent to the term polymer. Nevertheless, all plastics are polymers, but not all polymeric materials are plastics. Polymers can be divided into three different groups : a) elastomers (rubbers), b) plastics and c) fibers. This classification is made based on their physical features, elastic modulus and degree of elongation.

There are five high volume groups of plastics : polyethylene (low density PE-LD, linear low density PE-LLD and high density polyethylene PE-HD), polypropylene (PP), polyvinyl chloride (PVC), polystyrene (solid-PS, expandable-EPS), polyethylene terephthalate (PET) and polyutherane (PUR) [3]. Counted together, they constitute 80% of all the plastic demand in the world in 2011.Plastics have a wide variety of combinations of properties. Some are very rigid and brittle, while others are flexible, exhibiting both elastic and plastic deformations when stressed and sometimes experiencing considerable deformation before fracture. The biggest market shares belong to polyethylene (29%), polypropylene (19%) and polyvinyl chloride (11%). Figure 1.1 shows worlds plastic demand divided by different types of plastics in 2011.

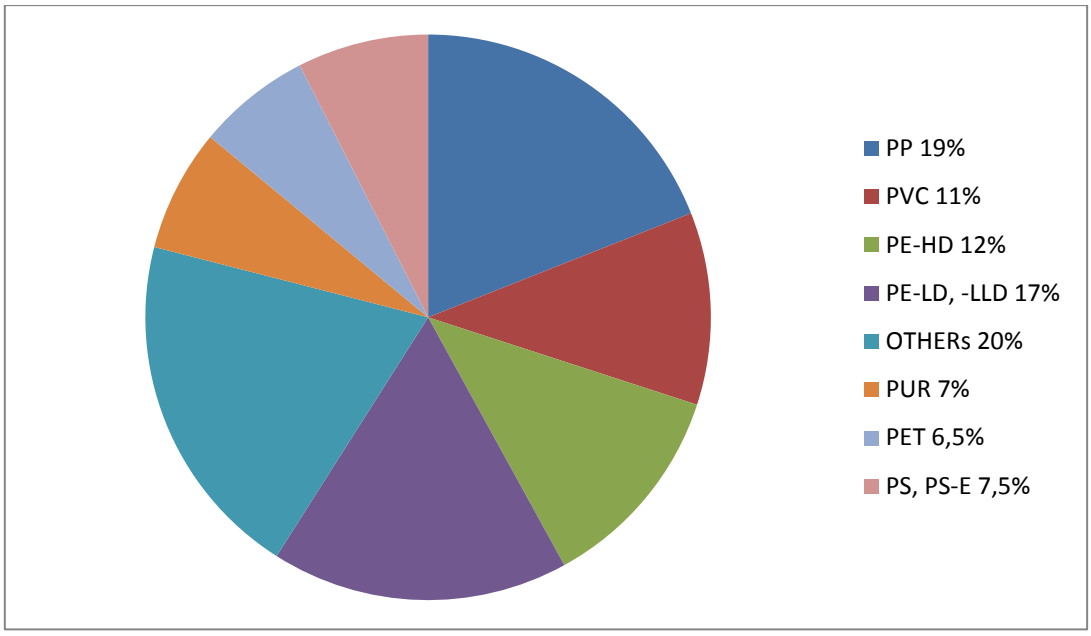

Figure 1.1 – World plastics demand by different types of polymers in 2011 [3]

Polypropylene

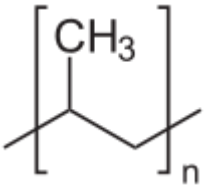

does not present stress-cracking problems and offers excellent electrical and chemical resistance at higher temperatures. While the properties of PP are similar to those of polyethylene, there are specific differences. These include a lower density, higher softening point (polypropylene has melting point at 160 °C, while polyethylene softness at 100 °C) and higher rigidity and hardness.

In this work all of the experiments will be carried-out on two different samples of polypropylene: with and without additives. Additives are intentionally introduced to enhance of modify some of the plastic's properties and, thus, render the polymer more serviceable. Typical additives include filler materials, plasticizers, stabilizers, colorants and flame retardants.

Order of Stability

Thermal stability of polyolefins is affected by branching, with linear polyethylene the most stable and propylene with one alkyl group on the second place. The order of stability is illustrated below:

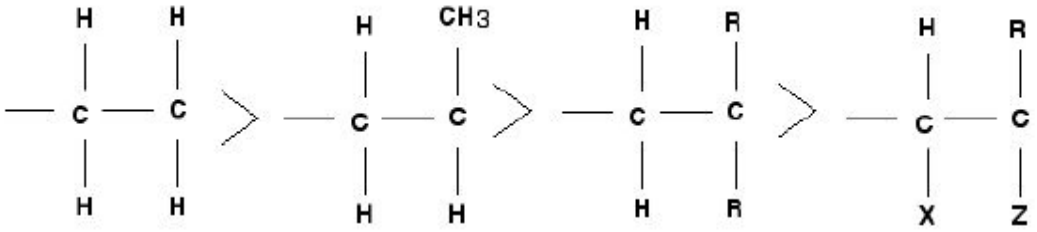

Taken from Beyler and Hirshler, 2001 [4]

Where R is hydrocarbon group larger than a methyl group.

1.2.2 Plastic Consumption

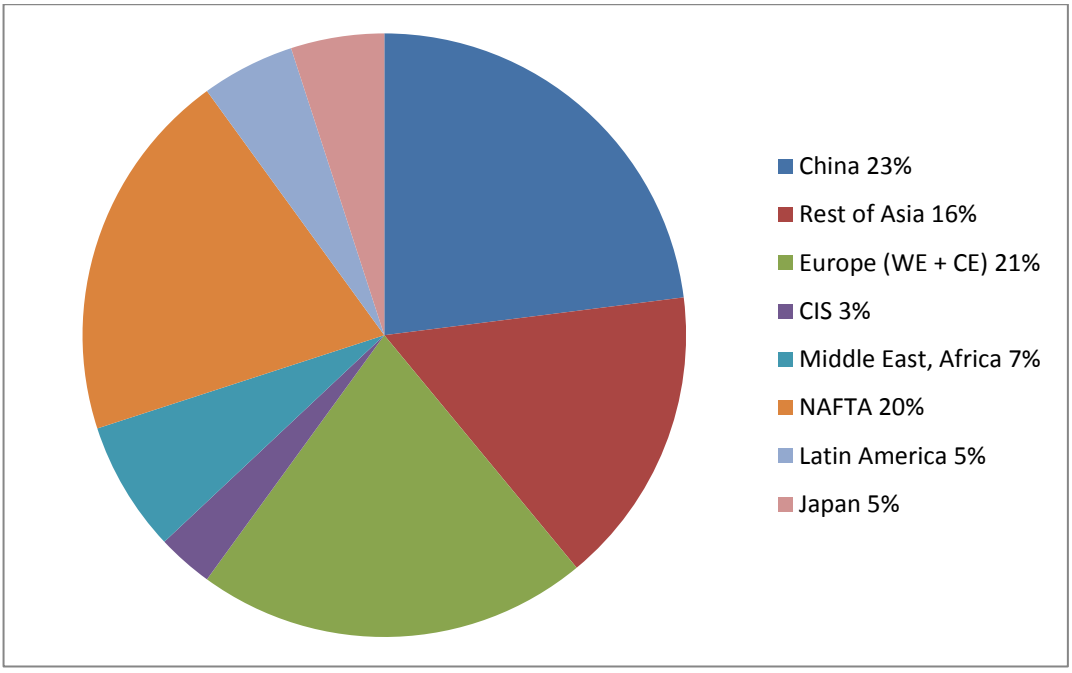

Figure 1. 2 - World plastic production by produced countries, in 2011. [3]

Taking into account the wide range of applications and relatively low cost of plastics, both consumption and plastic waste generation is increasing rapidly. According to the Association of Plastics Manufacturers in Europe [3], in 2011 total worldwide production of plastics was equal 280

million tones, with 21% produced in Europe, being Germany is major producer (12 million tons), followed by Italy (7 million tons), France (5 million tons) and Spain (3,8 million tons) (see Figure 1.2.)

1.3 Environmental impact of plastic waste

The most common Municipial Solid Waste (MSW) methods to manage plastic waste are recycling, when possible, incineration and landfilling. The latter method are considered to produce a negative impact on the environment since, due to its chemical inertness and low biodegrability. it requires substantial time for plastics to break down in the landfills and so it occupies a large space of the landscape. From another point of view, there are incineration methods in which energy is recovered, but this methods produce mayor amounts of toxic substances which are harmful to ambient.

Recycling and reuse of plastics has the benefit of decreasing the quantity of plastic wastes which ends up in landfills. Still, the overall recovery of plastics for recycling is relatively small. In accordance with Association of Plastics Manufacturers in Europe (APME) [3], in 2011 of the 58 million tons of plastics used in Europe 25,1 million tons were recovered and 14,9 million tons were reused (59%), through recycling or energy recovery. Remaining 20,2 million tons were sent to the disposal facilities (41 %).

1.3.1 The economic and environmental factors

There is a need to develop new sustainable answers for plastics management than incineration and disposal at landfills. Plastic waste recycling can provide an opportunity to collect and dispose plastic waste in environmentally friendly way, and also it could be converted into resource of energy Both thermal and catalytic degradation of polymers are hopeful alternatives which allow plastic conversion into gaseous and liquid hydrocarbons.

From an economical point of view, used plastics are considered to be an important source of chemicals, mainly hydrocarbons, and an energy source. The calorific value of the hydrocarbons from polymers are similar to values obtained from fuel oils and even higher than coal (see table 1.1) [4].

Table 1. 1 - Calorific values of plastics compared with conventional fuels [6]

Fuel or waste	Calorific Value [kcal/kg]
Coal	6000 - 8000
Heavy oil	9500
Wood/paper	4300
Plastics (polyethylene)	11000
Typical municipial wastes	1000-1500

1.4 Depolymerisation of Polypropylene

1.4.1 Pyrolysis of Polypropylene

Plastic pyrolysis concerns thermal degradation at temperatures between 400 to 600 °C in an inert atmosphere. As mentioned previously, one of the plastics that is present in large quantities in municipal solid waste is polypropylene. Many studies on polypropylene degradation appeared in literature.[47-54]

During the pyrolysis plastics are heated at a high temperature when their macromolecular structures are broken, which gives rise to smaller molecules yielding a broad range of hydrocarbons that can be used as fuels or chemicals. This is a possible solution for society concern for polymeric waste disposal and to preserve petroleum resources on top of protecting the environment.

On the other hand, this process requires a lot of energy according to heating to high temperatures and the poor quality of the products obtained make thermal degradation economically uninteresting. This method, however, can be improved by adding catalysts.

Several families of catalysts have been used for cracking the polymeric materials: zeolites, vermiculites.

1.4.1.1 Reaction Mechanism

Thermal cracking

As previously mentioned, the polypropylene structure is formed from a large number of the smaller molecules, monomers, that are joined together by bonds with a specific energy, giving rise to a long chain.

When the heat supplied exceeds bond dissociation energy, cleavage of the bonds can take place and long chain break into smaller fragments.

The backbone of the polypropylene is broken when all C-C bonds are with the same strength. Thus, the hydrocarbon chain breaks randomly and the products are in the form of different alkanes and alkenes of smaller size (see figure 1.3). The mechanism involved is probably a free radical chain mechanism (see figure 1.4). Formation of free radicals on the polypropylene chain causes the polymer to undergo scission leading to formation of saturated and unsaturated small molecules.

Polypropylenic fragment

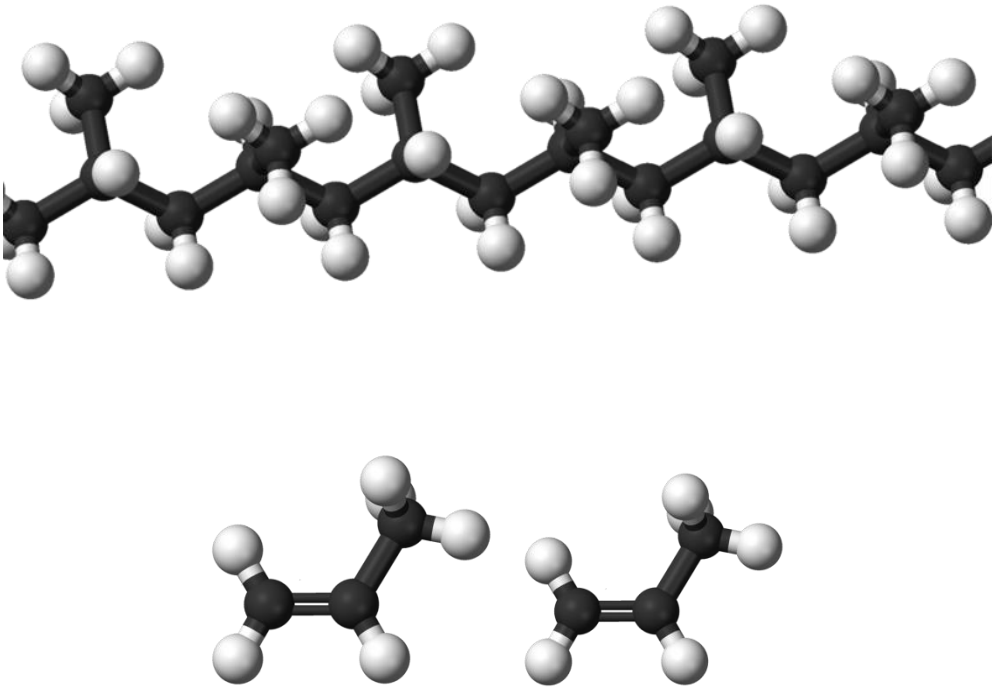

Figure 1. 3 - - Random depolymerisation [58].

Assuming that, initially, the covalent bond among two carbon atoms suffers random scissions, this will result in no mass loses but there will be some energy absorbed corresponding to endothermic process since some energy is needed for the bond to break. In homolytic scission two fragments are formed, having unpaired electron each; these fragments are called free radicals.

The overall reaction mechanism for the thermal degradation is described by the following succession of steps:

- **Initiation** occurring at random scission of the polymer chain and forming primary radicals Rp (1)
- **Propagation** leads to the release of olefinic monomeric parts formed from primary radicals by β-scission and producing predominantly propene (2)
- **Hydrogen chain transfer reaction** may happen as intermolecular or intramolecular (depending on low or high temperatures) processes.

The intramolecular hydrogen transfers leads to more stable secondary radicals. The subsequent β-scission of secondary radicals cooperates with the propagation step of the radical chain mechanism since a new primary radical is formed in this process. In addition, during this process C-C bond homolysis the formation of olefins occurs.

Furthermore, secondary radicals may also be formed through hydrogen abstraction by an intermolecular transfer reaction among a primary radical and a polymeric fragment. In this reaction, formation of alkane occurs.

- **Termination** happens in a bimolecular mode with the coupling of two primary radicals.

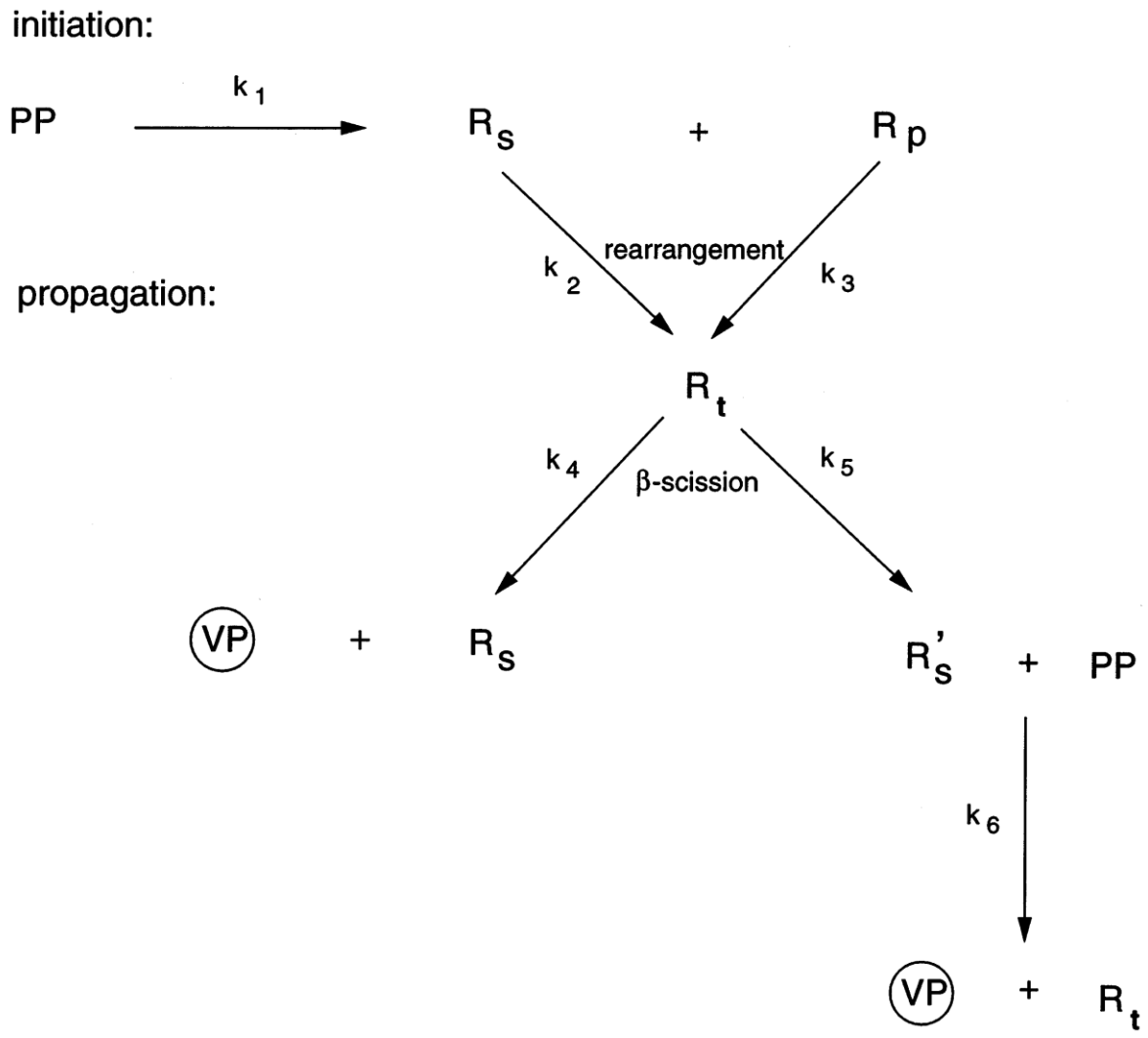

PP	polypropylene	R'_s	short secondary radical
R_p	primary radical	R_t	ternary radical
R_s	secondary radical	VP	volatile product

Figure 1. 4 – Radical mechanism of the thermal degradation of polypropylene. Adapted from H.Bockhorn et al. [8]

Catalytic cracking

As mentioned before, the catalysts have significant role in pyrolysis process. Pyrolysis in the presence of a catalyst usually requires less energy than it is needed in the non-catalytic process. Consequently, the catalysts allows the reduction of the processing temperature that leads to a decrease in energy consumption; at the same time it improves the output quality and the corresponding yield (both gas and liquid hydrocarbons used as fuels).

Comparing to thermal degradation, which usually occurs via free radical mechanism, catalytic degradation occurs by carbocations, which consist of hydrocarbon ions carrying a single positive charge.

As an example, the mechanism of catalytic pyrolysis of polyethylene was proposed by Buekens and mainly, this process evolves: (1) initiation, involving a carbenium ion formation by proton addition to unsaturated bond or an hydride abstraction from a saturated one; (2) propagation, where chain cleavage yields an oligomer fraction by β-scission; (3) isomerizaton; (4) aromatization.

1. **Initiation:** occurring on some defect sites of the polymer chain. For example, an olefinic linkage could be converted into an on-chain carbenium by adding a proton.

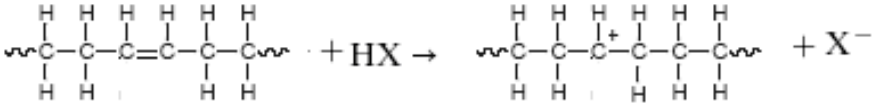

Next, the polymer chain is broken through β-scission.

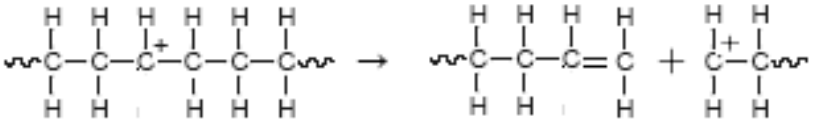

This step of degradation may also take place through random hydride ion abstraction by low-molecular-weight carbenium ions (R^+). After that, the formed on-chain carbenium ion undergoes β-scission.

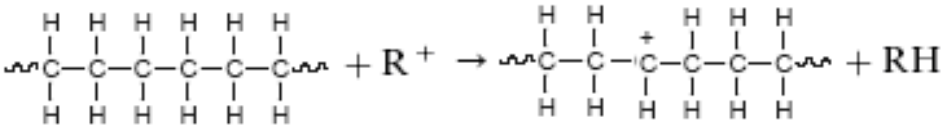

2. **Propagation:** in this step molecular weight of the main polymer chain can be lowered through successive attacks by acidic sites or another carbenium ions and chain cleavage, yielding oligomer fraction. Later cleavage of the oligomer fraction by direct β-scission of chain-end carbenium ions leads to gas formation and liquid fraction.
3. **Isomerization:** the carbenium ions intermediates can undergo rearrangement by hydrogen or carbon atom shifts, leading to double-bond olefin isomerization.

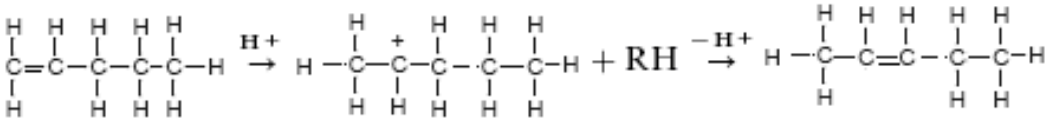

Another important isomerization reactions are shift of methyl group and saturated carbons isomerization.

4. **Aromatization:** some part of carbenium ion intermediates can undergo cyclization. For instance, when hydride ion abstraction first takes place on olefin at a position several carbons taken from the double bond, olefinic carbenium ion is being formed.

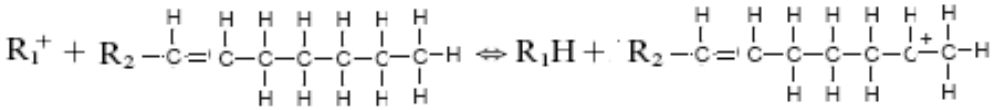

This ion can undergo intramolecular attack on the double bond that provides a route to formation and cyclization of aromatics.

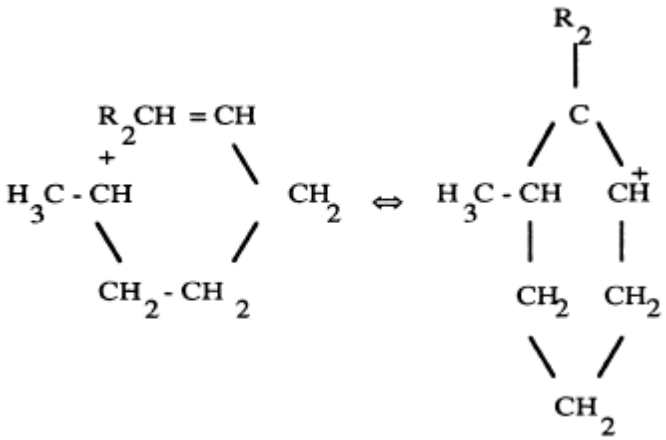

Acid sites with enough acidic strength can also induce C-C bond protolytic scission.

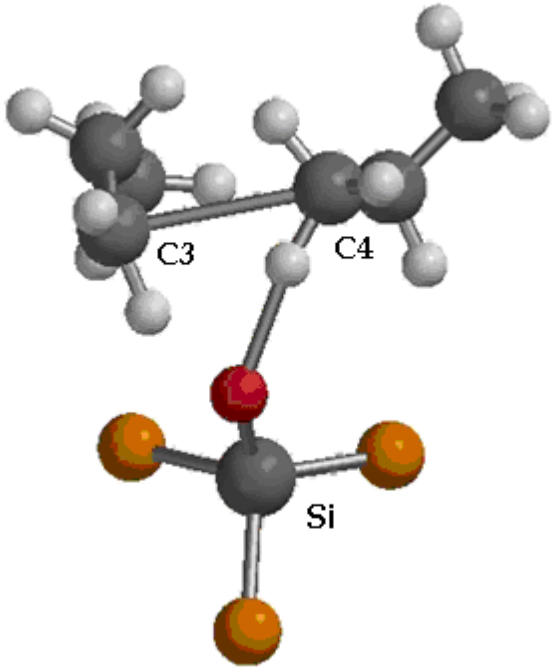

Figure 1. 5 - Presentation of the state structure transition of n-hexane for catalytic cracking reaction.

Figure 1.5 presents the transition state obtained for the protolytic cracking reaction for n-hexane over a presentation of an acidic zeolite site. This simulation was based on a transition state using the *PC SPARTAN PRO*® program [reference].

Kinetic studies

To gain an overall understanding of the reaction processes, it is important to know the kinetics of degradation using kinetic modeling modeling [27-36] and gas phase product analysis. [21,22,23,24,25,26]

Nevertheless, since the process mechanism is very complex and depends on many factors, kinetic parameters of polypropylene pyrolysis presented in the literature are significantly different. The reason for differences between these values are connected to the diversity of mathematical expressions adapted as kinetic equations and kinetic analysis methods applied in different studies. Also, the use of different types of material samples (influence of the average molecular weight and molecular weight distribution) and operating conditions (temperature, pressure, heating rates etc.). This results in a variation of reaction order found by many researches with the objective of elucidating the pyrolysis kinetics of polypropylene between 0 and 1.[55-57]

1.4.2 Thermogravimetric (TG) and Differential Scanning Calorimetric (DSC) analysis

There are many technologies and reactors [37-44] than can be used to pursue the reaction, but due to the nature of the pyrolysis, thermogravimetric analysis (TGA) is widely considered as a useful technique to study the degradation processes and its kinetics.

However, with TGA the reaction is only detected after it has occurred, when the products are becoming small enough to evaporate into the gas phase leading to the decrease of observed polymer mass. Taking this into account, the kinetic models used to described the process are basically based on the weight loss analysis curves obtained during thermal gravimetric analysis of the polymeric samples. A similar objection can be raised when only the gas-phase products are analyzed. Anyhow, it is possible to follow the reaction from the start, since each bond of polymer that is broken consumes some amount of energy. By measuring the heat flow into the sample during the reaction (for example using DSC), it is possible to measure the rate of breaking bonds even if this leads to species that are still too heavy to evaporate and do not produce any significant mass losses and, thus, cannot be seen in the TG signal.

Example of the studies that use DSC technique was performed by Conesa [36] and Marcilla [45,46] who have written the energy balance for the sample in the apparatus but applied different approaches to describe the various heat consumption terms.

1.5 Catalysts

1.5.1 Zeolites

Zeolites are crystalline aluminosilicates with composition expressed by the formula

$$Mx/n(AlO2)x(SiO2)y.zH2O$$

Where: M stands for the compensating cation with palence n, z is the water contained in the zeolite, x+y represents number of tetrahedrous SiO_4 and AlO_4^- and y/x is the atomic ratio Si/Al, which can chang)e from the minimum value of 1 to infinite (in accordance with Loewenstein rule).

Describing the structure of zeolites, there is a extensive three-dimensional framework where oxygen atoms links the tetrahedral sites. This resulting in microporous structure, with a big probability of channels and cavities being formed. As a consequence each type of zeolite has a different structure.

Primary individual structural element of zeolite is a tetrahedral silicon or aluminium atom, connected with four oxygen atoms (SiO_4 and AlO_4^-) (figure 1.6)

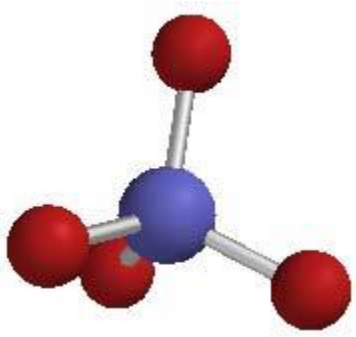

Figure 1. 6 - - Draft of a tetrahedral T-site - T-atom (blue) connected to four oxygen atoms (red) [11]

Consequently, zeolite frameworks are usually anionic, due to the existence of trivalent aluminium atoms in an essentially siliceous structure; this negative charge is neutralized with cations which are located within the framework, to obtain electrical neutrality. These cations are usually exchangeable, under appropriate conditions and if the counter cation present in the structure is a proton, then the zeolite will have acid characteristics.

Acidity of zeolites

In acid zeolites, the activity is determined by the Brønsted and Lewis sites, mainly because the presence of aluminium in the zeolite framework.

To describe the acidity of zeolites is necessary to distinguish the nature and strength of the acid sites. Hydroxyl groups are typically associated with Brønsted acid sites while the tri-coordinate aluminium and the cationic species correspond to Lewis sites.

Brønsted acid sites are inducted when the negative charge in the lattice is neutralized by a proton. Brønsted sites are considered to be able to protonate reactant molecules, generating carbocations that will then suffer a series of transformations to became products. These acid sites are created when Si^{4+} is isomorphically substituted by a trivalent metal cation, for instance Al^{3+}; when this substitution occurs a negative charge is generated in the zeolite framework [10]. If the cation introduced to compensate this charge is a proton, Brønsted acid site is created, due to the following scheme :

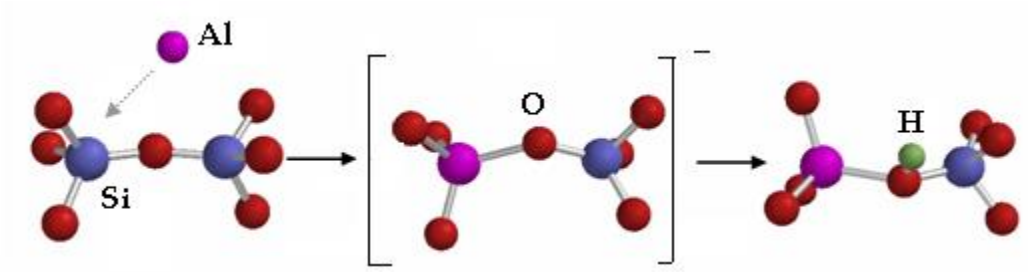

Figure 1. 7 - Brønsted acid sites formatted in zeolite. [11]

The major factors that affect the acid strength are the Si/Al ratio (or silica to alumina – SiO_2/ Al_2O_3 ratio) and the nature of other species that may be present in the framework or microporous volume. As an example, if the isomorphic substitution involves other tri-valent species, in place of Al^{3+}, the acidity increases as follows $Al^{3+}>Sc^{3+}>Ga^{3+}>Fe^{3+}>>B^{3+}$.[12]

The Si/Al ratio is connected to the total number of the Brønsted sites which is equivalent to the number of tetrahedral aluminium atoms present in the framework balanced by the presence of proton. According to the Lowenstein rule Al-O-Al linkages in this frameworks are not possible, because an oxygen atom cannot bond with more than one aluminium atom. Thus, the maximum Si/Al ratio in zeolite framework is equal 1. Due to this, when there is an increase in the value of Si/Al ratio, number of Brønsted sites decreases because the fraction of Al atoms also decreases. Brønsted acid sites concentration can be lowered by dehydroxylation and/or dealumination [13]. However, it should also be mentioned that when the Al/Si ratio decreases, although the number of acid sites decreases, their acid strength increases. Thus, to obtain an optimized acid catalyst it is important to have a balance between number and strength of the acid sites.

However, there are other kinds of acid sites present in zeolites, Lewis sites which are generated by the presence of cationic species. In the case of zeolites, the Lewis acidity may be associated to extraframework alumina species (EFAL) and to aluminium species that are removed from the framework during high temperature hydrothermal treatments. [14]

Lewis acid sites can be associated with different surface species: $Al(OH)_2^+$, $Al(OH)^{2+}$, AlO^+, $[Al_2O_2OH]^+$, $[Al_2O]^{4+}$, AlOOH, $Al(OH)_3$ and $\equiv Si^+$ may be observed in the zeolite structure [11,12].

1.5.2 Vermiculites

Vermiculite is the geological name given to a group of hydrated laminar minerals which are aluminum-iron magnesium silicates. They have the appearance of mica, and can be found in various parts of the world. When processed for horticultural use, the mineral is subjected to intense heat, expanding it into accordion-shaped granules with countless layers of thin plates.[15]

The most basic structure of the vermiculite is identical to the micas and to talc: a 2:1 silicate sheet composed of two flat layers of silica and alumina - the tetrahedral layers, that are joined together in a layer composed of apical oxygen atoms, magnesium, iron, and hydroxyl molecules - the octahedral layer. Silica layer can be seen in Figure 1.8. According to the AIPEA Nomenclature Committee, the tetrahedral sheet is composed of continuous two-dimensional corner-sharing tetrahedra $[TO_4]^{4-}$ involving three basal oxygens and the apical oxygen. The tetrahedral sheet has a composition of $[T_4O_{10}]^{4-}$ where T = Si^{4+}, Al^{3+}, Fe^{3+}. The apical oxygens form a corner of the octahedral coordination unit around larger octahedral cations. The octahedral sheet consists of two planes of closely packed O^{2-}, OH^- anions of octahedra with the central cations Mg^{2+} or Al^{3+}. The smallest structural unit contains three octahedral sites and one empty site. Complex formula of vermiculites can be written as :

$$(OH)_4,Mg_6[(Si, Al)_8,O_{20}] \text{ [[16]}$$

Where the different parts are separated by water layers.

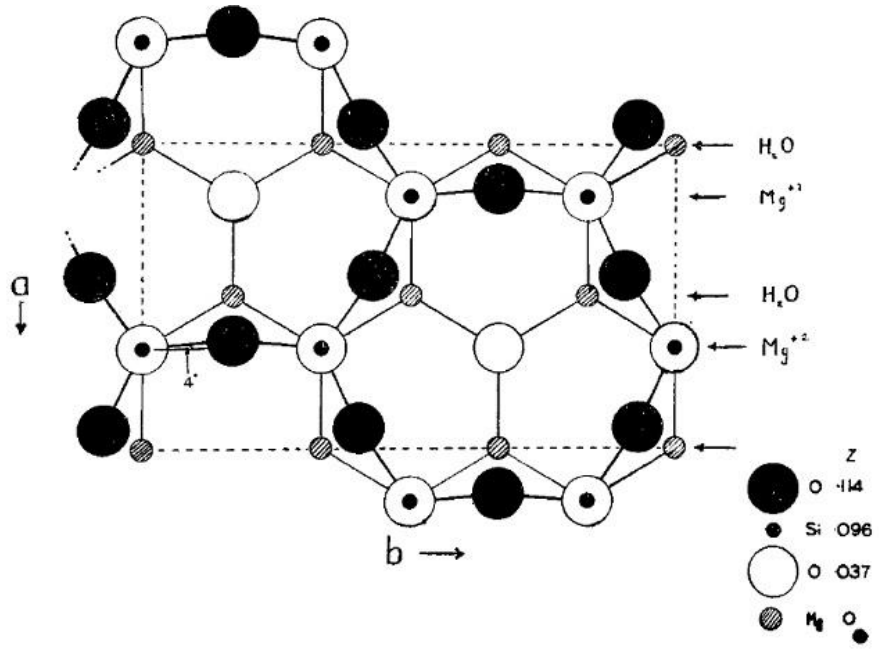

Figure 1. 8 - The scheme of the silica layer in vermiculite.

The vermiculite structure includes water interlamellar layers that are subjected to the hydration and dehydration processes. The hydration properties are controlled by the interlayer cations Mg^{2+} and minor amounts of Ca^{2+}, Na^{+}, and K^{+}. The cation radius and charge influence the degree of hydration state in the interlayer and the stacking layer sequences. The hydration state of vermiculite is defined by the number of water layers in the interlayer space. The basal space of Mg-vermiculite was measured as 0.902 nm for zero-water layer, 1.150 nm for one-water layer and 1.440 nm for two water layer hydration state.

Typically, the pH of the vermiculites is close to neutral, but in some cases, with the presence of associate carbonate compounds, the reaction is alkaline. Thus, the pH of vermiculite can change within a range from 6 to above 9.5. Also, depending on how this mineral is processed (exfoliated or expanded), the pH of the expanded particles can also change.

Vermiculites vary in their chemical composition, and this influences their morphology, surface acidity and cation exchange capacity. Many of them contain significant amounts of transition metal cations, for example iron, which is a typical component of vermiculites. To increase the acidity of vermiculites, which is a very desirable property in polymer degradation reactions, an acid-activation has to be performed. Acid treatment produces an increase in surface area and acidity. During this operation exchangeable cations are replaced with H ions, and leaching of Al and other cations out of both octahedral and tetrahedral sites occurs, but leaving the SiO_4 groups intact largely. The detailed preparation of catalysts from vermiculites is described in chapter 2. [17]

1.5.3 Montmorillonites

Montmorillonites are clay minerals broadly used in industrial processes, because of their properties: large specific surface area and high thermal stability. In this work montmorillonites, extracted from bentonite, were used. They belong to the smectities group and have packing of 2:1, consisting of two silica tetrahedral sheets with central alumina octahedral sheet (as it can be seen in figure 1.9). Oxygen atoms bind to these sheets. The layers are continous in a and b axis directions and are stacked one above other in c direction; the degree of order dependent on the smectite clay mineral kind. There can be moderately isomorphic substitutions varying on the kind of mineral.

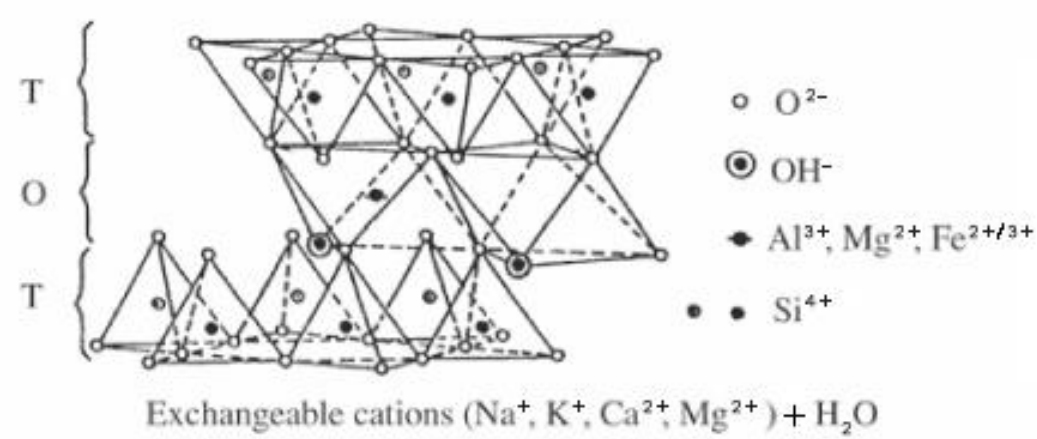

Figure 1. 9 - Montmorillonite structure. T – tetrahedral sheet, O – octahedral sheet [5].

Bentonite is obtained from the substitution of Al^{3+} for Mg^{2+} in the octahedral layer [19], resulting in the following molecular formula :

$$Mx^{+} (Si_8)^{IV}(Al_{4-x}\ Mg_x)^{VI}\ O_{20}(OH)_4$$

Where: M^{+} is the interchangable cation.

The parameters of montmorillonite (surface area and high termal stability) are related to the changes produced in the crystal structure by isomorphic substitutions. These substitutions take places both in a tetrahedral and octahedral layers, producing a negative charge density in the crystal structure. Also, some treatments, that modify this structure of crystals, for example cation exchanges,

thermal and mechanical treatments can add some other properties such as compression strength, swelling degree, resistance to degradation, etc. [18]

All of these properties have a significant importance in industrial processes. In oil industry, montmorillonites are used as absorbents to remove pollutants in suspension from products in the fractional distillation of crude.

Similar to vermiculites, acid treatment changes some properties of montmorillonities. It extends the surface and alters the pore size distribution by removing aluminium and other ions from the octahedral layer. Activation with hydrochloric acid also modifies the clays surface by replacing the exchangeable ions with hydrogen and aluminium. [20]

CHAPTER 2. EXPERIMENTAL PROCEDURES AND APPARATUS

This chapter describes methods and techniques used to study the degradation of polypropylene. Firstly, there is a specification of the polymer and the catalyst material used. Secondly, the method interposed in the Thermogravimetric (TG) and Differential Scanning Calorimetric (DSC) analysis accompanied with the method for analyzing gas products from TGA and DSC apparatus during the polymer degradation will be reviewed.

2.1 Polymer Materials

The materials used in this work were both polypropylene with and without additives, kindly supplied by Borealis. Polypropylene with additives in powder form had, according to the supplier, molecular weight Mw~290 000 (α=Mw/Mn~20); and show melt flow indexes MFI5=0.39/10min; MFI21=11.8g/10min; MFI21/MFI5= 30 while the polypropylene without additives samples were in form of pellets and show a molecular weight, Mw~376 000 (Mw/Mn~23).

2.2 Catalyst Materials

1) Zeolites

- HZSM – 5
- HY
- BEA
- H-BEA

2) Vermiculites

- Transition metals supported in vermiculites as catalysts, namely zirconium, alumina, copper and silver.

3) Montmorillonites

- Mt_6OAlCu
- K10 + Cu^{2+}
- K10 Al Ag^{+}

2.2.1 Original catalysts specifications

The specifications of the original zeolites used in this work are summarized in table 2.1. This information was given by the supplier or by the researchers.

Table 2. 1 - Specifications of the original zeolites used in this work.

Zeolite type	**Si/Al molar ratio**	**BET Surface Area (m^2/g)**	**Crystallite size (μm)**	**Pore size (Å)**
HZSM-5	15	425	0,5-1	5.6 x 5.6
HY	32	780	0.5-1	7.4 x 7.4
BEA	150	620	1-2	7.4 x 6.4
H-BEA	23	680	1-2	

These catalysts differ in Si/Al molar ratio, BEA catalyst has the highest molar ratio of this components and HZSM-5 has much more lower one. Zeolite BETA, three-dimensional high- silica zeolite, currently receives much attention as a potential catalyst in the degradation processes. In addition to its Brønsted acidic properties it displays Lewis acidity as well.

2.2.2 Preparation and Characterization

Catalysts used in this work have been previously prepared and characterized by other researchers.

- **Zeolites**

H-ZSM-5 catalyst was prepared by calcination at 773K during 8 hours under a flow of dry air. The HY zeolite used in this work was obtained from NaY by ion exchange with a 2M aqueous solution of NH_4NO_3, performed at 373K during 1 hour, followed by calcination at 773K under air. Zeolite BEA was prepared by partial dealumination by treatment with nitric acid solution. H-BEA catalyst is an acidic form of the BEA catalyst. Both were calcinated in 773K in static air.

- **Vermiculites**

Vermiculite from Brazil was used as a starting material. The particle size fraction < 40 μm was obtained by milling in a planetary mill for 20 min and sieving by a sieve with a pore size of less than 40 μm.

Vermiculites with transition metals : Cu^{2+},Zr^{2+} and Ag^{+} were prepared by introducing 5 % of the adequate metal by incipient wetness impregnation.

Samples V/Ag and V/Cu were prepared from vermiculite (V) and the 0.1M aqueous solution $AgNO_3$ and 0.1 M $Cu(NO_3)_2$, respectively, at the ratio of 1:10 (grams of vermiculite: millilitre of solution), and the suspension was shaken for 24 hours.

Catalyst VH Cu^{+} was prepared by acid activation with 20% hydrochloric acid for 60 min. Next, 5 % of copper was introduced by incipient wetness impregnation. The same way were the VH Ag^{+} prepared, but instead of copper, 5% of silver was introduced.

- **Montmorillonites**

Mt_6OAlCu catalyst is a sample of montmorillonite extracted with bentonite. It was activated for 60 min with 20% hydrochloric acid. Next, it was supported by aqua hydroxo aluminum cations and 5% copper was introduced by incipient wetness impregnation.

KlO Cu^{2+} it is a commercial acid-activated montmorillonite catalyst, supplied by Aldrich company. In this catalyst, 5% of the copper were introduced by incipient wetness impregnation.

KlO Al Ag is also commercial acid-activated catalyst supplied by Aldrich. It was prepared by aqua hydroxo aluminium cations and 5% of silver was introduced by incipient wetness impregnation.

2.3 Acid strength distribution

The acid strength of the several catalysts, representatives of each group was determined by temperature-programed desorption (TPD) of ammonia.

The catalyst samples were saturated with ammonia by placing them in a container with an ammonium solution; this solution staturated the atmosphere within the vessel with gaseous ammonia and was kept at 40 ºC for 12 hours.

After saturation, the desorption experiments were carried out in a DSC/TG apparatus, using a quartz pan. Samples were heated up to 600 °C with a heating rate equal 10°C. Blank experiments, were no ammonia was adsorbed were also performed in order to obtain baselines.

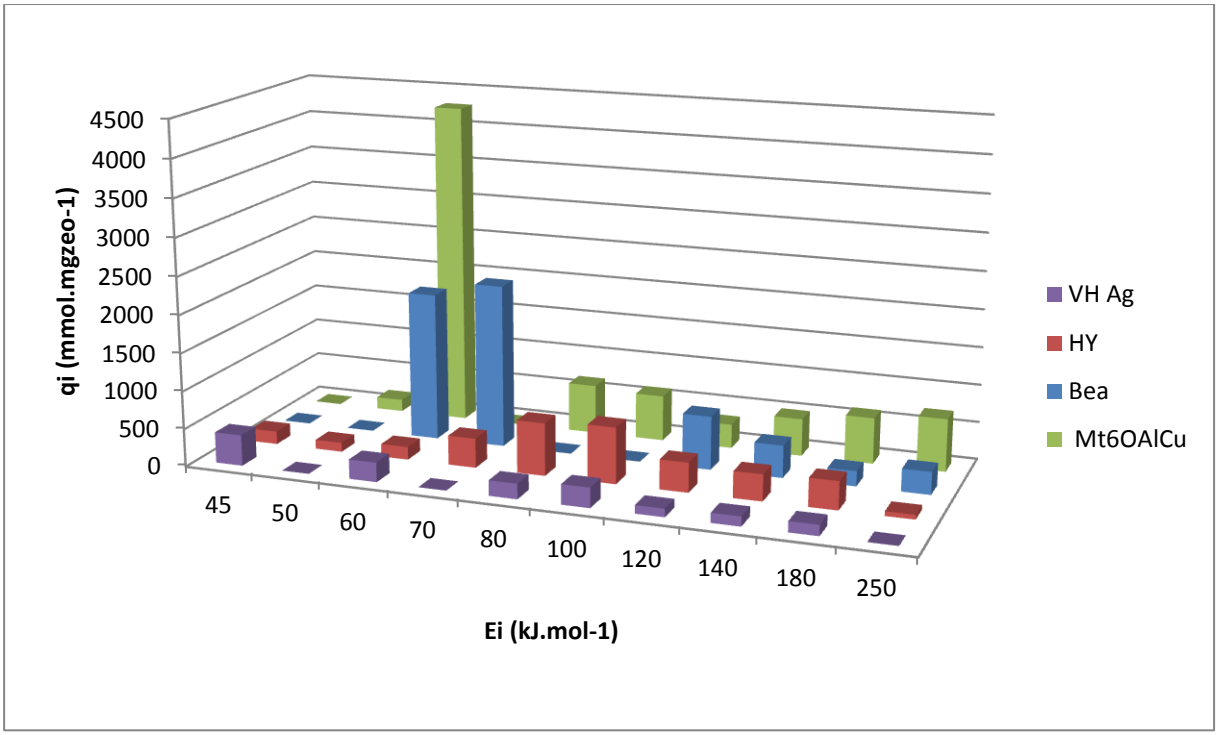

Figure 2. 1 - Acid sites distribution for catalysts : VH Ag^{+}, HY, Bea, Mt_6OAlCu.

The acid strength distribution was obtained for four different catalysts: Mt_6OAlCu (Montmorrilonites), HY and Bea (zeolites) and VH Ag^{+} (Vermiculites), from the NH_3-TPD by a numerical deconvolution method [59]. This method assumes an irreversible ammonia desorption process with first order kinetics and with no interactions between acid sites of different acid strength. Experimental data are fitted into Eq.1

$$-\frac{dq}{dt} = \sum_i KE_i \cdot e^{-(\frac{Ei}{RT})} \cdot q_{Ei} \quad \text{with} \quad K_{Ei} = \propto \cdot e^{\beta \cdot E_i} \qquad \text{(Eq.1)}$$

where E_i is the energy activation of the desorption of ammonia and K_{Ei} is corresponding pre-exponential factor. Parameters α and β depends on the structure of catalyst.

The results obtained for the NH_3 desorption from each type of acid site q_{Ei} are depicted in figure 2.1. As we can see, zeolite HY present broad distribution of acidity, with desorption energy levels from 70 to 180 kJ mol^{-1}. The distribution shows the biggest amount of with strong acidic sites with energy levels between 80 and 180 kJ mol^{-1}.

In figure 2.1 distributions for other catalysts are also depicted. Vermiculite VH Ag^{+} has very small amount of strong acidic sites and only some weak acidic sites, with desorption energy level equal to about 60 kJ mol^{-1}. Catalyst Mt_6OAlCu shows a broad distribution of acidity, with desorption levels from 80 to 250 kJ mol^{-1}. It also presents a large amount of weak acidic sites with desorption energy 60 kJ mol^{-1}.

Another zeolite, Bea, shows similar results to the HY. It has significant values of strong acidic sites with energy levels from 120 to 250 kJ mol^{-1}, as well as a big values of weaker acidic sites, with desorption energy levels equal 60-70 kJ mol^{-1}. High values of the desorption energies at levels 50 – 70 kJ mol^{-1} for the Mt_6OAlCu and Bea catalysts can be explained due to the fact that there was some quantities of water which were also desorbed, apart to NH_3.

2.4 General Gases specifications

Nitrogen	Air Liquide (>99.995%)
Hydrogen	Air Liquide (>99.9990%)

2.5 Thermogravimetric (TG) and Differential Scanning Calorimetric (DSC) analysis

2.5.1 Sample preparation

All of the TG/DSC experiments were carried-out in a TA Instruments SDT 2960 simultaneous DSC-TGA apparatus. Before the runs, nitrogen flow was maintained through the system for 30 min to purge all the air from it. This flow rate was maintained during the experiments.

The PP samples, pure or along with the catalysts were placed in quartz TG pan and the thermal degradation was analyzed. The PP/catalyst mixture was prepared at room temperature in order to obtain 15-25 mg of mixture. The quantity of catalyst used was approximately 1-3mg, depending on the experiment.

2.5.2 Temperature Profile

The first part of the experiments was carried out using dynamic conditions, by raising the temperature with different heating rates. The runs were performed under nitrogen with continuous flow rate 80ml/min, with various heating rates: 10,20 and 40 °C/min. The temperature was going up from

room temperature up to 600 °C. This temperature was maintained for an additional 10 min. Experiments with various heating rates were performed for non-catalytic degradation and for degradation with H-ZSM catalyst. For the rest of experiments with catalyst the heating rate was equal 10°C/min.

.

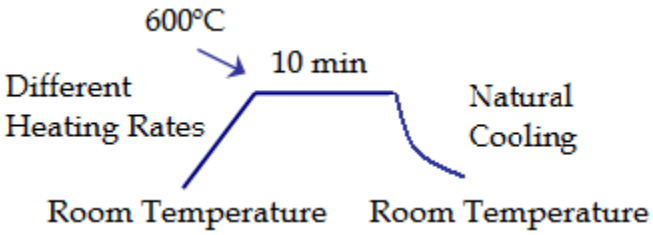

Figure 2. 2 - Temperature profile for the polypropylene degradation.

At the end of each run, the oven was cooled down and a second run was performed under the same conditions, to obtain the baselines. This was done because DSC signal is very sensitive to the layout of the pans inside the oven.

2.5.3 Equipment

The thermal analysis simultaneous DSC-TGA equipment consisted of three components:

1. Sensitive recording balance.
2. Furnace and associated controller/ atmosphere management.
3. Computer with special data system and recorder.

Instruments presented in the Figure 2.3 include:

a) Furnace bellow
b) Balance
c) Computer
d) Gas line (N_2)
e) Gas flow measurer

Figure 2. 3 - DSC-TGA equipment.

Figure 2. 4 - Loading sample pans on balance arm; sample pans in the open oven.

To evaluate the data received from TGA/DSC, the software TA Universal Analysis 2000 was used. This data software is a helpful tool for analysis of data obtained from TGA/DSC equipment SDT 2960.

The data collected during the experiments were stored in the in the computer connected with the equipment. This data is compatible with the TA Universal Analysis 2000 software and can be analyzed using it but it can also be exported so that it can be processed further.

CHAPTER 3. THERMAL PYROLYSIS OF POLYPROPYLENE

In this chapter, the thermal degradation of polypropylene with, and without additives in an azotium atmosphere was studied using the thermogravimetry (TG) and differential scanning calorimetry (DSC)[60,61].

Analysis included the influence of the temperature and the heating rates. TGA/DSC analyses were conducted in non-isothermally way. The conditions were dynamic, at three different heating rates: 10, 20, and 40 °C /min. During the heating, measurement of changes in weight and heat flow were performed in order to investigate the behaviour of the sample as a function of temperature.

A kinetic model was applied which allows a simultaneous correlation of the signals obtained from TG (thermogravimetric curve that can be known also as a weight loss curve) and DSC (heat flux curve obtained from the difference in heat absorbed by the reference and by the sample pan), under dynamic conditions and allows further insight into the chemical process. Fitting this model to experimental results made possible to estimate some kinetic and thermodynamic parameters.

3.1 Polypropylene with additives

3.1.1 Dynamic conditions at three different heating rates

3.1.2 DSC/TG analysis

The results obtained from the DSC/TG analysis on PP with additives sample for four different heating rates are shown in figure 3.1. Picture (Figure 3.1b) shows the curve corresponding to the DSC signal with two endothermic peaks. The first one corresponds to the melting of the polypropylene sample, which occurs at 170 °C/min and has no significant weight change, as it can be seen in Figure 3.1a. The second endothermic peak occurs at higher temperatures and is related with polymer degradation. This peak is accompanied by a weight loss. The start of the second DSC signal is due to the energy which is given to the sample when the bonds in the polymer begin to break. This breakage of the bonds in the polypropylene produces increasingly lighter products that will become sufficiently small to be volatile at the temperature of reaction and will evaporate from the pan, leading to the easily observed mass losses as well as to additional consumption of energy.

The temperature at which polypropylene with additives suffers thermal degradation when using heating rates between 10 and 40° C/min are in the range of 458 to 488°C . The list with all temperatures at which the maximum rate of heat consumption occurs for this process are presented in table 3.1 for the different heating rates.

With increasing heating rates, all the temperature maxima shift towards higher temperatures (see both table 3.1 and figure 3.3), because of a variety of factors and in accordance with other experimental observations. The most important one is related to a kinetic effects. In a single run along with the temperature increasing, the rate of chemical and physical processes taking place also increase in an exponential form, which leads to an increase in heat and mass loss rates. Nevertheless, when sufficient material is transformed, the decrease in the amount of available species compensates this increase in the reaction rate, which leads to the maximum observed in the rate curves. This maximum shifts to higher temperatures as the heating rate is increased, because at higher heating rates there is less time for the reaction to occur, and the depletion of the reactants takes place at higher temperatures.

Seeing that the rate of the reaction increases faster in the case of the higher heating rates, in figure 3.3b it is possible to observe that the highest peak corresponds to the highest heating rate used (40°C), as well that the lowest peak corresponds to the lowest heating rate (10 °C/min).

The effect of the heat transfer may also become more important when the heating rates increases, as well as the dynamics of the equipment may also become more important for very high heating rates. When the heating rate is too high, the sample temperature might not be linear with the increase of the furnace temperature.

There is also an effect that is noticeable at the higher heating rate – the degradation peak appears to be split into two different peaks, which may indicate that the chemical reactions occurring have two different pathways with different activation energies.

Table 3. 1 - Degradation temperature for the polypropylene samples obtained from TGA/DSC results.

Sample	$T_{degrad.}$ (°C)
PP with add.10°C/min	458,9
PP with add. 20°C/min	477,2
PP with add. 40°C/min	488,2

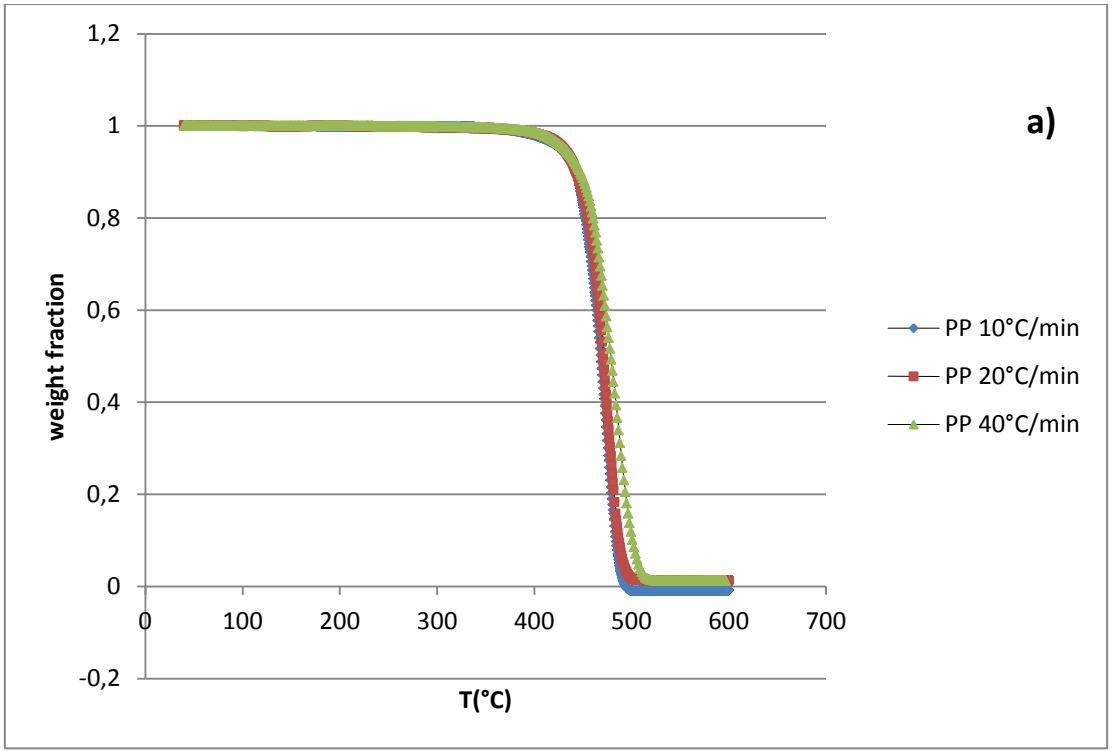

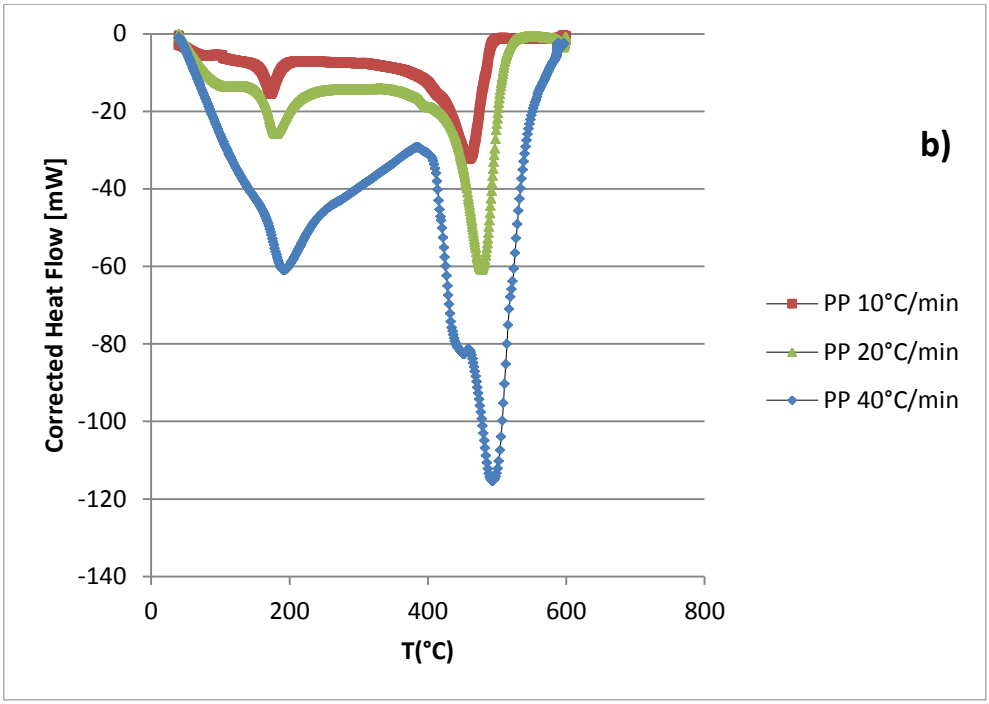

Figure 3. 1 – TG (a) and Heat Flow (b) curves obtained from the degradation of PP with additives at different heating rates (see chapter 2 for additional conditions).

3.1.2.2 Kinetic model studies

The degradation process takes place by successive bond breakages. With every bond broken, a certain amount of energy is needed and this can be seen in the heat flow signal. However, the TG signal only records mass losses and not all bonds breakages are accompanied by losses of mass.

When relatively small molecules are formed, they will leave the system with the gas flow and then a mass loss is detected. The initial bond breakages will lead to the formation of relatively large molecules that will not be volatile. This will not result in any measurable weight change. For that reason. only the combination of DSC and TG will be able to provide a full look into the degradation process.

The formation of gas phase products involves two steps. The first one corresponds to the breakage of the bonds and production of smaller molecules and the second one corresponds to the evaporation of these smaller products. Each of the steps is associated with a different energy consumption. This information was used to build a computational model employed to interpret experimental results which were obtained.

The information used to develop the computational model was the material and energy balances to the number of bonds in the sample at each experiment. We assume that the

polypropylene molecules are long chain of alkanes, the number of C-C bonds per unit of mass, N will be given, for a very large n, by the limit of the expression

$$N = \frac{n-1}{14n+2} = \frac{1}{14} \qquad \text{(Eq.1)}$$

where n – the number of carbon atoms in the molecule. When n is very large, the number of C-C bond is close to 1/14 and it can be assumed that this is the bond density at the beginning of each experiment.

As mentioned above, C-C bonds are lost in two ways: one due to the cracking reactions, either thermally induced or by a catalyst. However, when a relatively small molecule is formed, it will evaporate into the gas-phase, carrying with it a certain number of still unbroken bonds. This corresponds to the second way that bonds will be lost from the PP sample. The average number of lost bonds per unit mass of evaporated material to the gas phase, at a given moment, is designated by α, . The balance to the number of bonds in the sample will be:

$$\frac{dN}{dt} = -k(T)N + \frac{dm}{dt}\alpha \qquad \text{(Eq.2)}$$

where dm/dt is the rate of mass loss. A first-order process is assumed in relation to bond concentration and $k(T)$ is the corresponding temperature-dependent rate constant, described by the Arrhenius law.

$$k(T) = k_{ref} e^{-\frac{E_a}{R}(\frac{1}{T}-\frac{1}{T_{ref}})} \qquad \text{(Eq.3)}$$

Where T_{ref} is a reference temperature chosen from the range of a significant weight loss (573K), E_a is the energy of activation of the reaction, and k_{ref} is the kinetic constant at the reference temperature (T_{ref}). This expression was used in this form for fitting objectives, to reduce parameter correlation.

Using the information above it is possible to estimate heat flow measured by apparatus, by performing an energy balance to the pan, assuming that the apparatus is able of correctly compensating the required flows. With this approach the heat flow will be given by:

$$Heat\ Flow = -mCp\frac{dT}{dt} - k(T)N\Delta H_{c-c} + \Delta H_{vap}\frac{dm}{dt} \qquad \text{(Eq.3)}$$

where m is the weight of the sample at a given time, that is obtained experimentally. C_p is the average heat capacity of the polymer, ΔH_{c-c} is the average C-C bond enthalpy and ΔH_{vap} is the average vaporization enthalpy per unit mass.

This expression can be fit to the experimental heat flow curve taken from the correction DSC curve after baseline. The fitting parameters are: k_{ref}, E_a, α, C_p, $\Delta H_{C\text{-}C}$ and ΔH_{vap}. For the latter three, initial values were obtained from the published data. The average number of bonds in the evaporated material, α, was taken as independent of time. In addition, response time of the heat sensor flow was assumed as finite and a first order dynamics was assumed for the sensor, for which the corresponding time constant was estimated during the fitting procedure.

The equation 2 was solved numerically, with use of the Euler method. The model parameters were estimated by a least-squares procedure, using the sum of the squares of the residues on the heat flow as the objective function, to be minimized:

$$O.F. = \sum_{all\ data\ points}\left[(Heat\ Flow)_{exp} - (Heat\ Flow)_{computed}\right]^2 \qquad \text{(Eq.5)}$$

The optimization procedure was carried out using 'Solver' tool from the Excel (© Windows) spreadsheet.

The model provides good fittings to the experimental data despite of the fact that some parameters, such as ΔH_{vap} and α were taken as independent of the temperature and time.

The fittings are plotted in figure 3.2 and all the kinetic parameters obtained by fitting the kinetic model for the pyrolysis of PP with additives at various heating rates are listed in table 3.2.

Table 3. 2 - Model parameters obtained by fitting the kinetic model for the thermal degradation of PP with additives at different heating rates

Heating rates (°C/min)	10	20	40
K (300ºC) (min^{-1})	$5{,}43 \times 10^{-4}$	$2{,}42 \times 10^{-4}$	$1{,}22 \times 10^{-4}$
E_a (cal/mol/K)	30000,12	30005,7	40804,1
$\Delta H_{C\text{-}C}$ (mJ/mmol)	20001,55	20001,27	22695,12
ΔH_{vap} (mJ/mg)	248,68	256,51	15986,07
α (Bond mole.g^{-1})	0,0212	0,0294	0,5914
C_p (mJ/mg/K)	2,6	2,75	1,75

Comparing the results obtained for thermal degradation of PP with additives at three different heating rates, we can observe that activation energy of the process is increasing with increasing heating rates. This observation is similar to other TG data described in literature [32,34]. As explained above, this can be due to the main factors like kinetics of degradation itself, suggesting that mechanism of PP decomposition depends on the heating rates. We can conclude that apparent specific reaction rate at the reference temperature decrease with increasing heating rates.

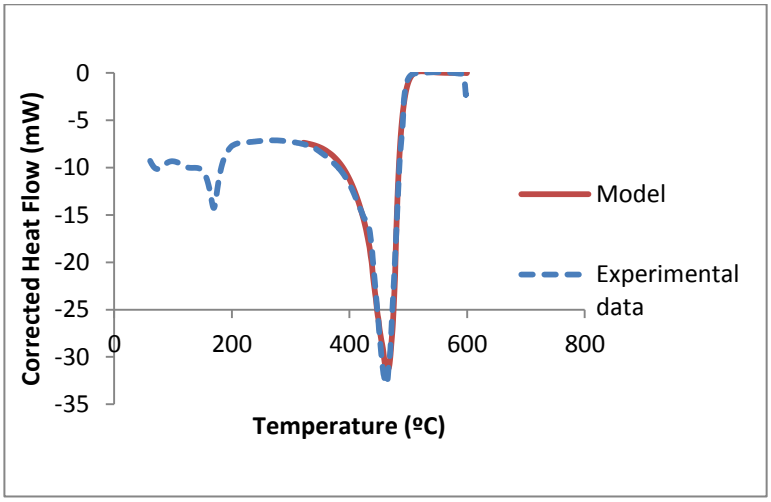

a)

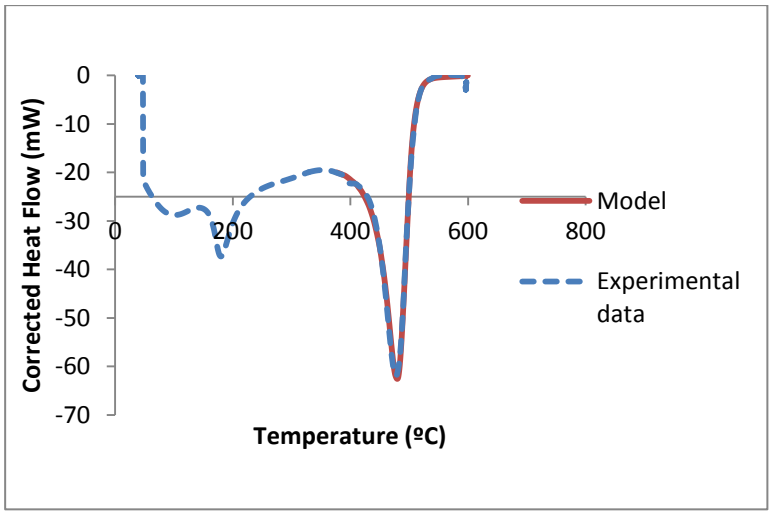

b)

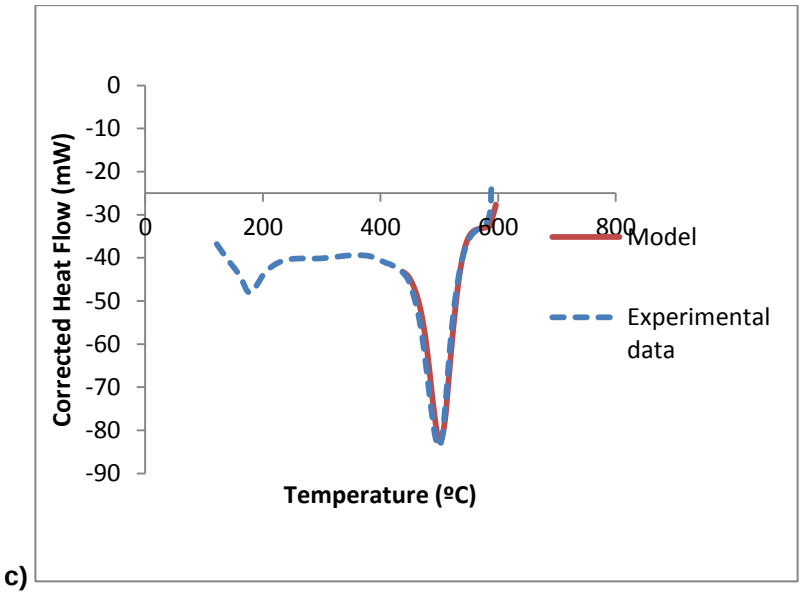

c)

Figure 3. 2 – Experimental and calculated heat flow curves for PP with additives – a) 10 °C/min, b) 20 °C/min and c) 40 °C/min.

When there is an increase in heating rates, the samples reach higher temperatures in a shorter time. Consequently, contribution of the process with higher activation energies increases in the overall process. This not only explains the increase in the apparent activation energy estimated with the model, that corresponds to an average activation energy over the entire range of temperatures that was covered. Also, it corresponds to the decrease in the apparent kinetic rate constant at the reference temperature.

The values of C_p, vaporisation and bond enthalpies estimated from the experimental data express some variations, probably because of the changes in the composition during the degradation process.

Analysing the model fitted into the experimental data, we can now have a more detailed look into the heat consumption processes occurring in the sample during the pyrolysis. The simultaneous use of TG and DSC signals allows us to have a clearer picture of the process. However, detailed kinetic model is rather more complicated since it involves the simultaneous modelling of all the chemical steps, involved in the formation of light products, and the physical steps, involved in the evaporation of the products from the pan.

3.2 Polypropylene without additives samples

3.2.1 Dynamic conditions at three different heating rates

3.2.1.1 DSC/TG analysis

The thermogravimetric analysis (TGA) and heat flow (DSC) curves for the pyrolysis of the samples of polypropylene without additives were tested for three different heating rates : 10, 20 and 40 °C/min. The results obtained are shown in figure 3.3. Decomposition of PP without additives in this range of heating rates vary from 459 °C to 494,7°C (see details in Table 3.3).

An single weight loss step characterizes the weight loss curves for this type of PP for different heating rates. The same comment was made for the weight loss curves obtained for PP with additives samples.

There is also an increase of the maximum of the heat flow curves to higher temperatures with the increasing heating rate (figure 3.3 and table 3.3), the reason is the same as one discussed in the previous subsection for PP with additives.

Another conclusion is that the highest area of the peaks corresponds to the highest heating rate (40 °C/min), and the smaller peak corresponds to the lowest heating rate used during the experiment (10 °C/min). With the lower heating rates there are two big differences when compare it with the higher heating rates: the weight loss start at lower temperatures and complete thermal decomposition occurs at lower temperatures. Also, using lower heating rates the complete time needed for the process is longer.

For the PP without additives decomposition starts at temperatures between: 459 °C, and the end of decomposition occurs at 494,7°C, for the heating rates in range 10-40 °C/min.

Table 3. 3 - Degradation temperatures for the Polypropylene without additives samples from TGA/DSC results, for different heating rates.

Sample	$T_{degrad.}$ (°C)
PP without add. 10°C/min	459
PP without add. 20°C/min	477,9
PP without add. 40°C/min	494,7

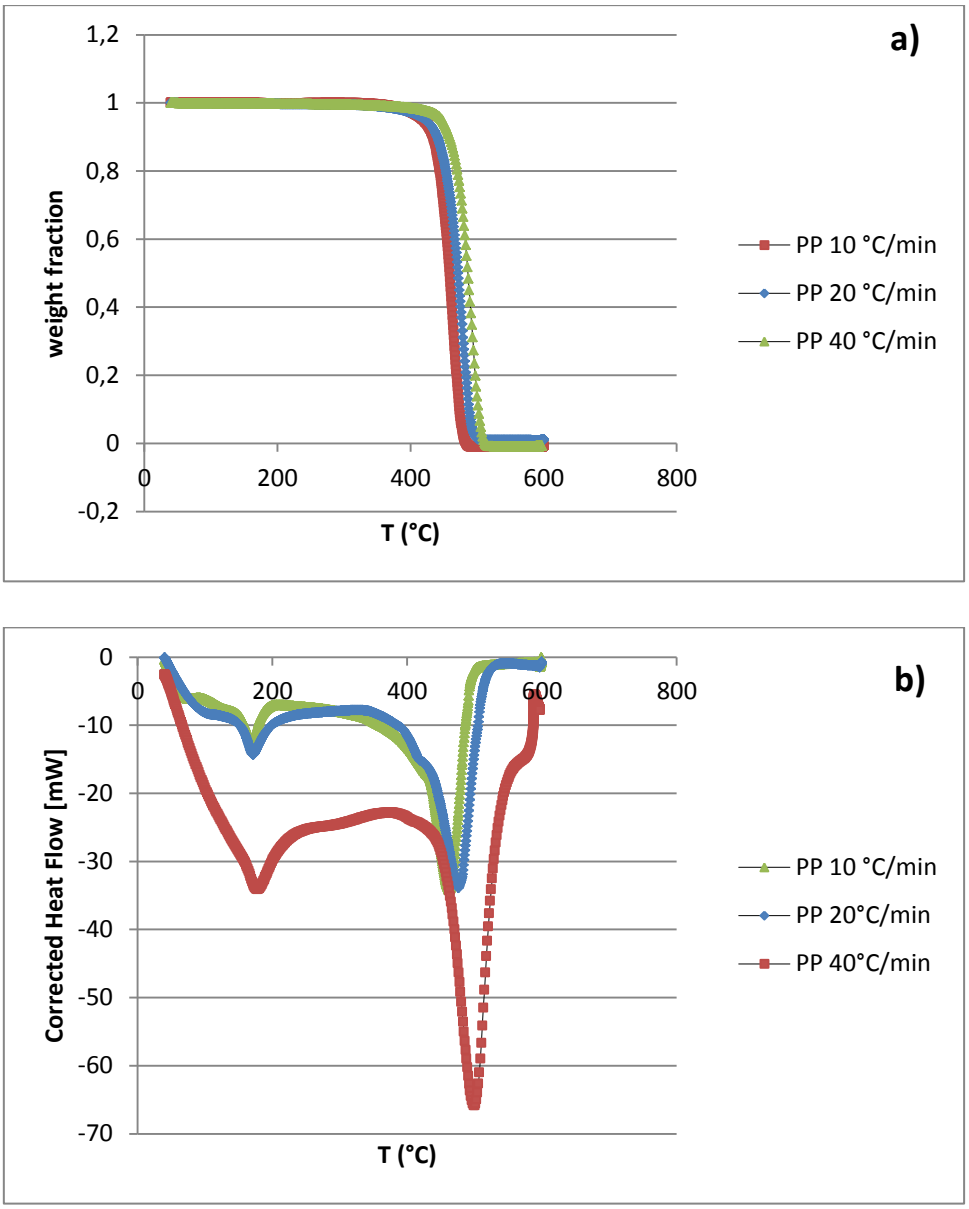

Figure 3. 3 - TG (a) and Heat Flow (b) curves obtained in the degradation of Polypropylene without additives at three different heat rates (see chapter 2 for additional conditions).

3.1.2.2 Kinetic model studies

As it was previously done in the case of thermal degradation of PP with additives the data obtained from the TG and DSC analysis recorded during thermal decomposition of PP without additives for the three heating rates, 10,20 and 40 °C/min, were used for estimation of the kinetic and thermodynamic parameters for the model shown above.

Table 3. 4 - Model parameters obtained by fitting the kinetic model for the thermal degradation of PP without additives at different heating rates.

Heating rates (°C/min)	10	20	40
K (300ºC) (min^{-1})	$5{,}98 \times 10^{-4}$	$1{,}05 \times 10^{-3}$	$1{,}22 \times 10^{-4}$
E_a (cal/mol/K)	30000,07	26000,12	40704,1
$\Delta H_{C\text{-}C}$ (mJ/mmol)	20001,56	27000,1	22595,12
ΔH_{vap} (mJ/mg)	242,17	249,99	15686,07
α (Bond mole.g^{-1})	0,0235	1,084	0,5814
C_p (mJ/mg/K)	2,46	1,69	1,75

In the figure 3.4, the experimental data are presented and compared with the theoretical curves. Kinetic parameters estimated for each experiment with different heating rate are shown in the table 3.4. The model gives good fittings to the experimental data.

By analysing table 3.4, it can be seen that for each heating rate there are different values of activation energy as well as energy of breaking bonds and evaporation. Similar results were obtained for the pyrolysis of PP with additives (see table 3.2).

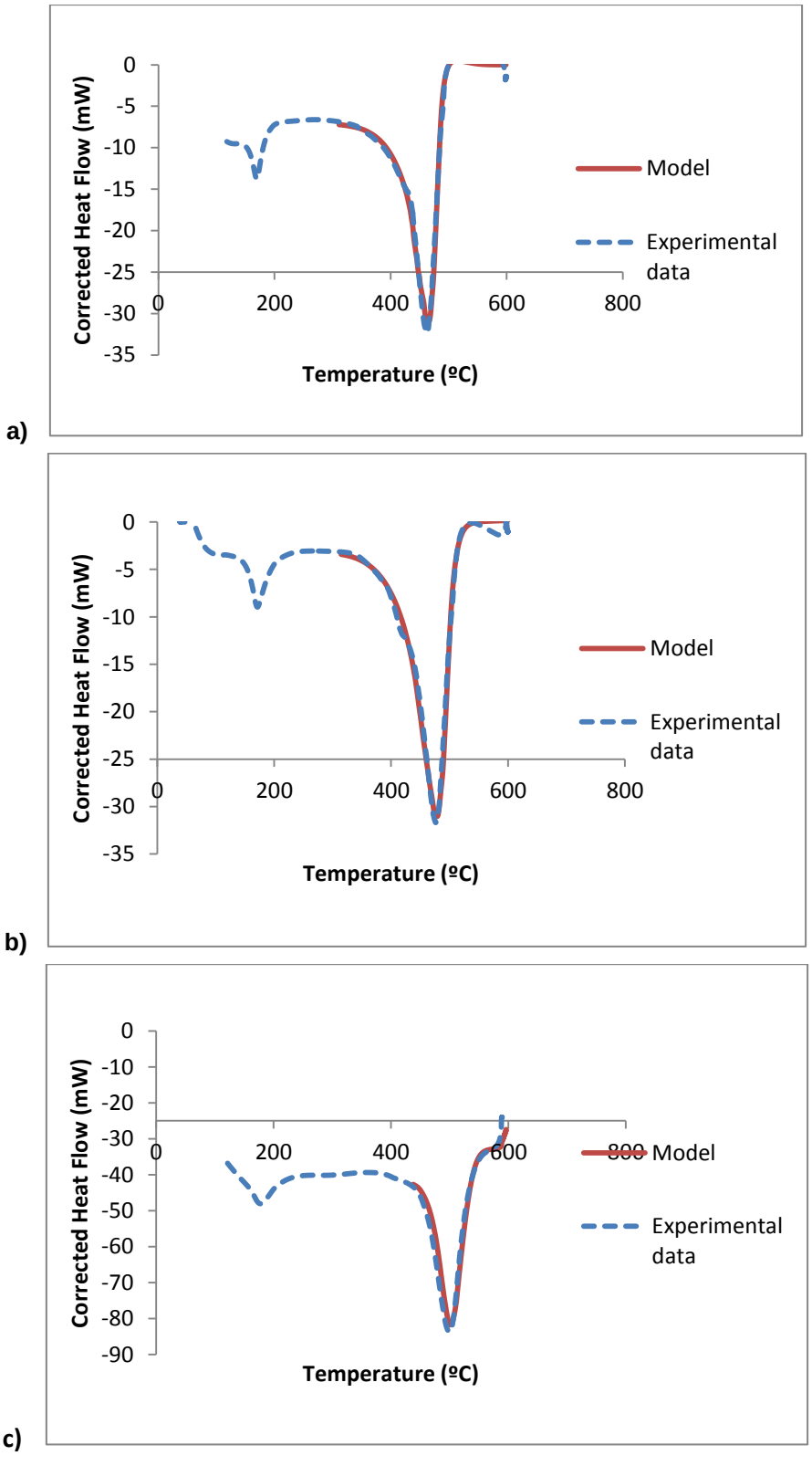

Figure 3. 4 - Experimental and calculated heat flow curves for PP without additives – a) 10 °C/min, b) 20 °C/min and c) 40 °C/min.

3.3 Effect of polypropylene type

3.3.1 Degradation temperature

As mentioned previously, at lower heating rates the weight loss starts at lower temperatures and complete process of thermal degradation occurs at lower temperatures when compare with process maintained with higher heating rates. This observation is made for both PP with and without additives.

The degradation temperatures for heating rates: 10, 20 and 40 °C/min are presented in figure 3.5 for the both types of polypropylene. The graph shows the dependence of the temperature at which the maximum of heat consumption occurs at different heating rates. The temperatures of degradation for polypropylene with and without additives at heating rates 10 and 20 °C/min do not differ a lot. There is a small difference between the temperature of degradation for the process at 40 °C/min heating rate – degradation of polypropylene with additives occurs at slightly lower temperature, indicating that the additives might play some role in the polymer degradation.

More detailed data can be found in tables 3.1 and 3.5 for the degradation processes of PP with and without additives, respectively.

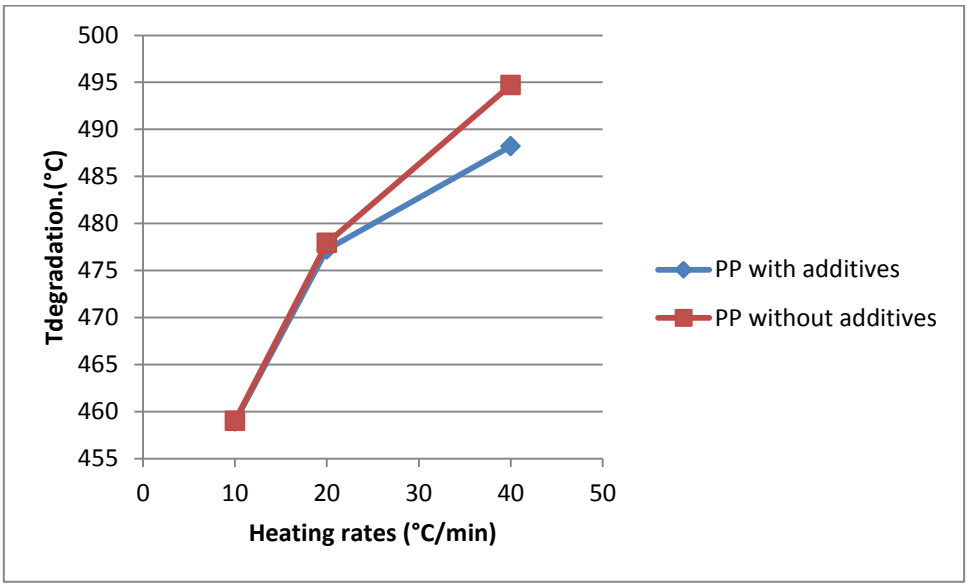

Figure 3. 5 – Decomposition temperature dependence on the heating rates for PP with and without additives.

CHAPTER 4. CATALYTIC PYROLYSIS OF POLYPROPYLENE

This chapter describes the results obtained for the catalytic degradation of polypropylene, using simultaneously Thermogravimetry (TG) and Differential Scanning Calorimetry (DSC) analysis.

Experiments are divided accordingly to the families of catalysts used: Vermiculites, Montmorillonites and Zeolites for the two first families all of experiments were carried-out with a heating rate 10°C, and for the group of zeolites the results were also obtained for 20 and 40 °C/min heating rates.

In the first part, there will be study on influence of Vermiculites on both type of polypropylene, comparing process to the thermal degradation without any catalysts. Influence of presence of transition metals also will be studied.

In the next part, there will be study on montomorillonities influence on degradation process on polypropylene with and without additives. Three catalysts chosen to study were: Mt_6OAlCu, K10 with transited copper and K10 with alumina and silver.

The last family of catalyst studied were the Zeolites, with four different catalysts: HZSM – 5 , HY, BEA and H-BEA.

At the end of chapter 4, activity of two the best representatives of families was further studied on pyrolysis of polypropylene with additives.

4.1 Vermiculites

4.1.1 DSC/TG analysis

As in the non-catalytic degradation, the results obtained in DSC-TGA run shows two endothermic peaks, from the DSC signal (see figures 4.1- 4.6). In previous chapter it was clarified that the first peak, which has no accompanying weight loss corresponds to the temperature when melting of the sample starts. It can be observed that the melting point remains constant for all of the experiments, being in the range: 165 – 172 °C, and the shape of the peaks are also similar. It can be concluded that the melting temperature is not influenced by the catalysts.

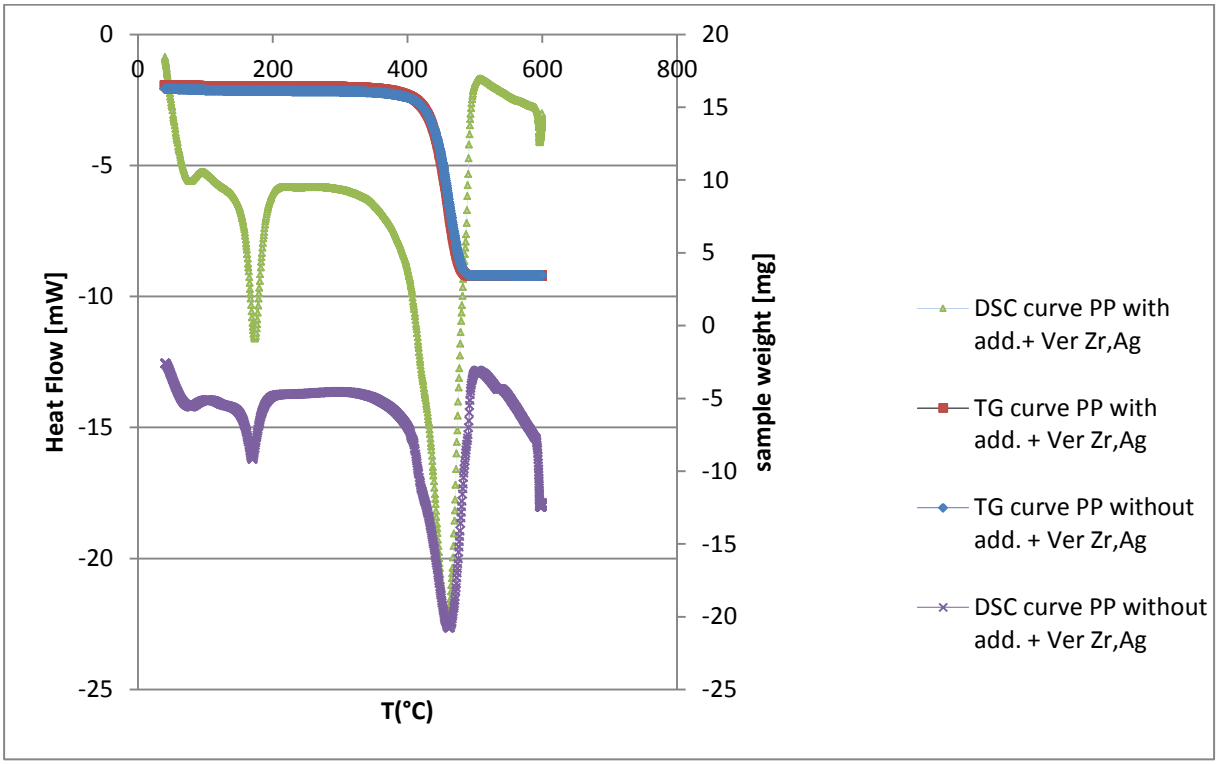

Figure 4. 1 - TGA and DSC curves obtained for the degradation of PP with and without additives, with presence of Vermiculite Zr, Ag^{+} (heating rate 10°C/min).

The second endothermic peak occurs at higher temperatures corresponds to the degradation of the polymer and is always associate by a significant weight loss (see figures 4.1 – 4.6 – TG and DSC curves, respectively). The temperatures at which the maximum of the heat consumption occurs are listed in table 4.1, in order to compare pyrolysis with catalysts and without. It can be seen that all types of vermiculites show little activity, leading to the negligible lowering of the degradation

temperature. This conclusion is being made for both types of polypropylenes, with and without additives, as can be observed in figures 4.1- 4.6 and table 4.1.

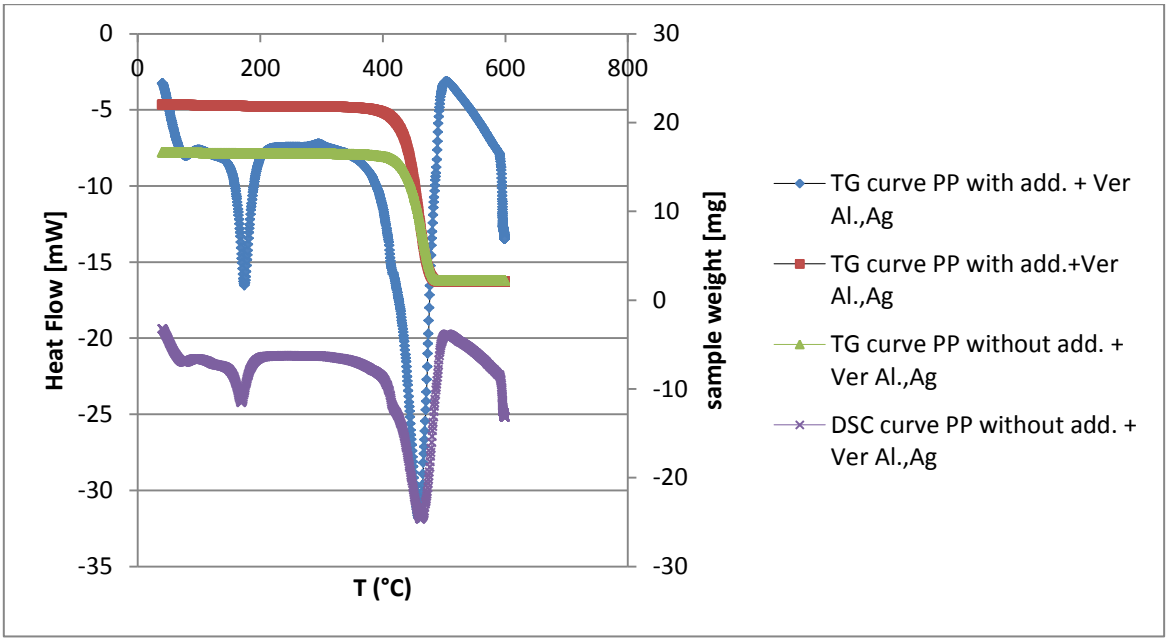

Figure 4. 2 – TGA and DSC curves obtained for the degradation of PP with and without additives, with presence of Vermiculite Al, Ag^{+} (heating rate 10°C/min).

As it can be observed in figures 4.1 – 4.6 there is no big difference in lowering the degradation temperature between experiments with vermiculites with transited metals (alumina, silver, zirconium and copper) and with the catalysts which were previously acidity activated (VH Ag^{+} , VH Cu^{2+}). Acidic activation causes an increase in acidity of vermiculites and an increase in surface area. For this reason, it could be predicted that VH Ag^{+} and VH Cu^{2+} are desirable catalysts for polymer degradation. Although, as it can be seen in figure 4.5 and 4.6, and also in table 4.1, there is no success in lowering the temperature of degradation.

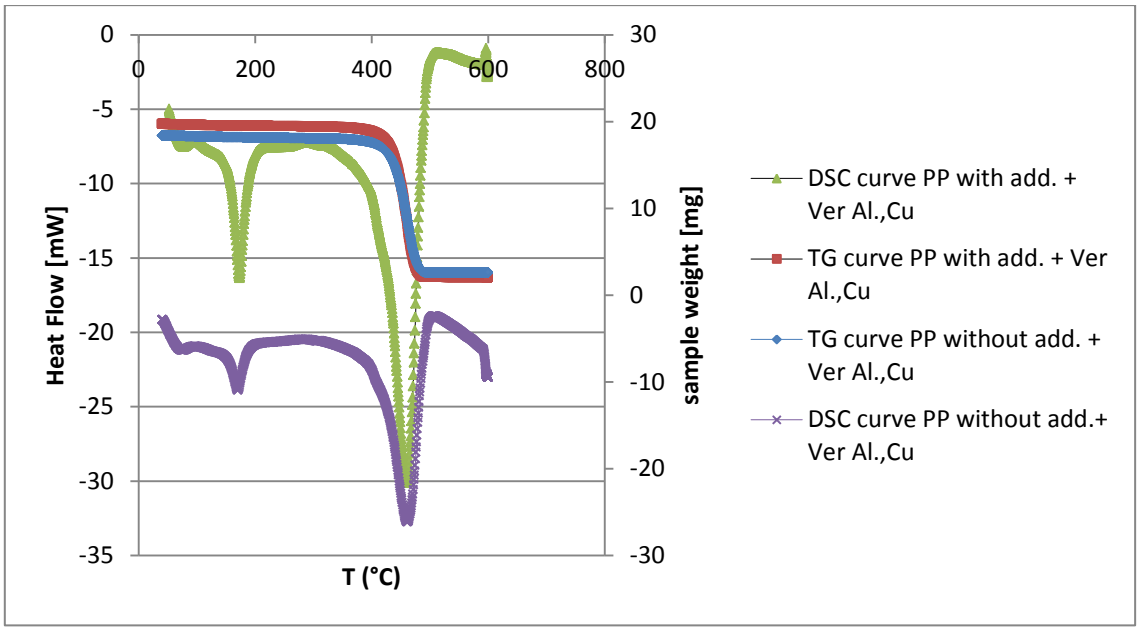

Figure 4. 3 - TGA and DSC curves obtained for the degradation of PP with and without additives, with presence of Vermiculite Al, Cu^{2+} (heating rate 10°C/min).

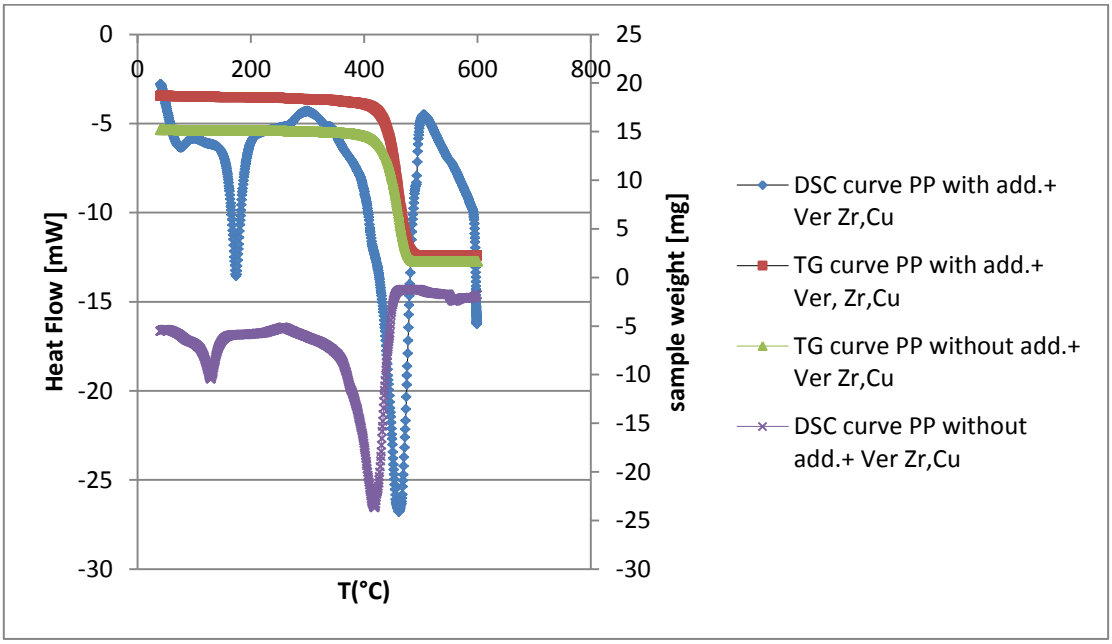

Figure 4. 4 - **–** TGA and DSC curves obtained for the degradation of PP with and without additives, with presence of Vermiculite Zr, Cu^{2+} (heating rate 10°C/min).

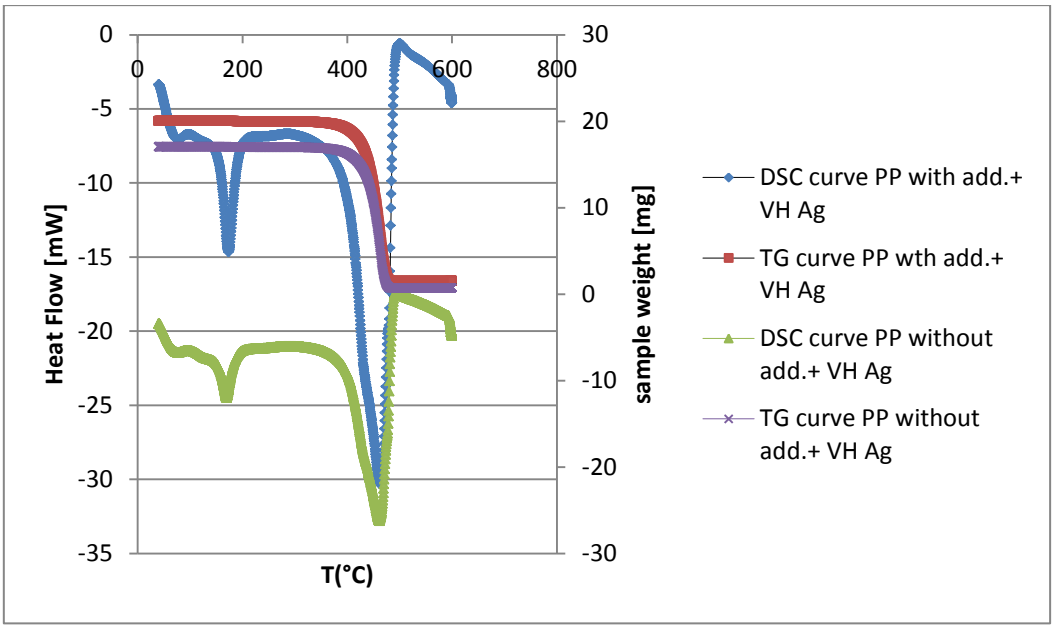

Figure 4. 5 – TGA and DSC curves obtained for the degradation of PP with and without additives, with presence of VH Ag^{+} (heating rate 10°C/min).

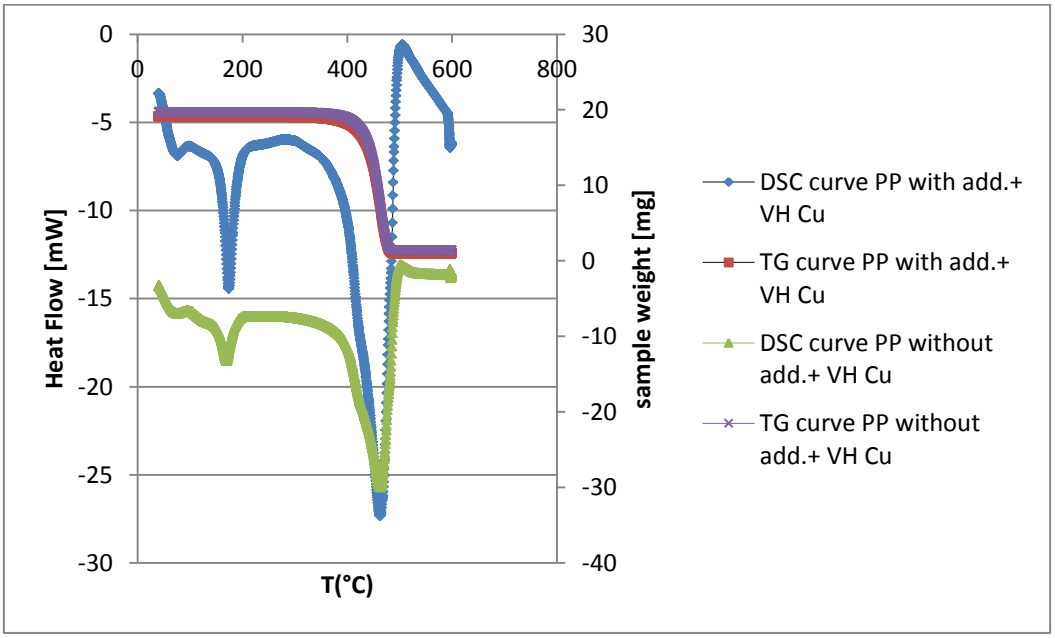

Figure 4. 6 - TGA and DSC curves obtained for the degradation of PP with and without additives, with presence of VH Cu^{2+} (heating rate 10°C/min).

In the table 4.1 temperatures of degradation are presented for all the experiments done with Vermiculites, as well with the temperatures for non-catalytic, thermal degradation of polypropylene

with and without additives. In both cases, presence of catalyst lowered the temperature of degradation for approximately 2-4 °C, which is not important from the economical point of view.

Table 4. 1 - Degradation temperature for PP with additives (a) and without additives (b) with catalysts Ver Zr,Ag^{+}; Ver Al,Ag^{+}; Ver Al,Cu^{2+}; Ver Zr,Cu^{2+}; VH Ag^{+} and VH Cu^{2+} obtained from TGA/DSC results. Heating rate: 10°C/min.

Sample	**$T_{degrad.}$(°C)**
PP with additives	458,90
PP with add.+ Ver Zr,Ag^{+}	453,76
PP with add.+ Ver Al,Ag^{+}	455,87
PP with add.+ Ver Al,Cu^{2+}	454,78
PP with add.+ Ver Zr,Cu^{2+}	455,08
PP with add.+ VH Ag^{+}	455,85
PP with add.+ VH Cu^{2+}	459,09

Sample	**$T_{degrad.}$(°C)**
PP without additives	459,00
PP without add.+ Ver Zr,Ag^{+}	456,33
PP without add.+ Ver Al,Ag^{+}	456,95
PP without add.+ Ver Al,Cu^{2+}	456,09
PP without add.+ Ver Zr,Cu^{2+}	455,08
PP with add.+ VH Ag^{+}	456,30
PP with add.+ VH Cu^{2+}	458,04

4.2 Zeolites

4.2.1 DSC/TG analysis

Applying the same methodology discussed in the previous sections the degradation of PP with and without additives was studied using zeolites as catalysts.

The first catalyst used was the HZSM-5, and for it, experiments were prepared for both types of polypropylenes, using heating rates 10, 20 40°C/min. For the HY, Bea and H-Bea all experiments were done with heating rate 10°C/min.

A comparison of the weight loss curves (TG curves) and the heat flow curves (DSC curves) are shown in figures 4.7 and 4.8 for the samples with polypropylene with additives, and 4.9 and 4.10 for the propylene without additives, respectively.

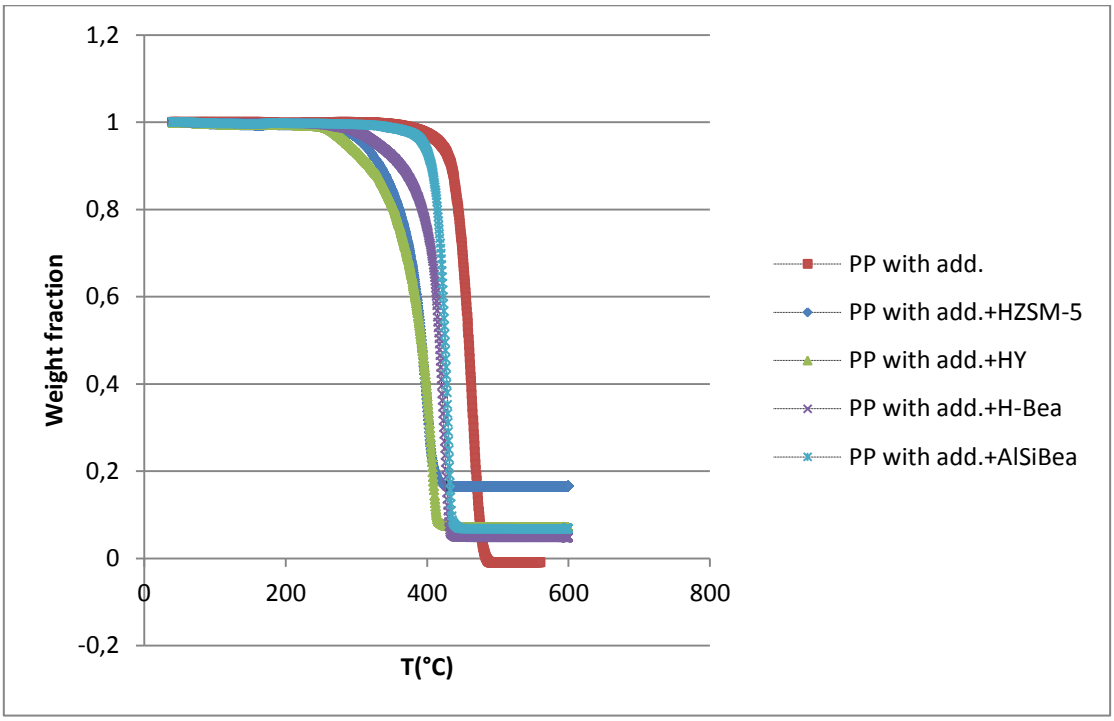

Figure 4. 7 – Weight loss curves (TGA curves) obtained in the degradation of PP with additives for non-catalyzed and catalyzed process with different zeolites.

In the chapter 3 it was explained that the first peak, which has no accompanying weight loss corresponds to the temperature of sample melting. This melting point remains constant for all the samples, approximately at 170 °C. In the case of zeolites, similar to vermiculites group, melting temperature is not influenced by the catalyst presence.

The second endothermic peak that occurs at higher temperatures, is accompanied by a weight loss (see figure 4.7-4.10). The temperatures of polymer degradation for polypropylene with and

without additives, with presence of zeolites are listed in Table 4.2. From the data presented in this table, it can be observed that presence of zeolites decreased the degradation temperature.

The zeolites' influence on the process can be explained because of the catalyst characteristics, and suggests that the acidic sites of the solid catalyst are the active catalytic sites in the polymer degradation process. The higher catalytic activity of the zeolites, when compared to the vermiculites (see table 4.1 and 4.2) in cracking reactions can be interpreted as a consequence of the combination of a stronger acidity and a higher accessibility of acid sites.

Another conclusion interesting to mention is that during the thermal degradation of polypropylene there is no formation of residues; after reaction the mass of sample tends to zero. With the presence of catalyst it is likely that some coke formation occurs, but at a very limited extent.

As mentioned in the chapter 1, zeolites have a large internal surface area with a large number of acidic sites, so it can be used for degradation of large molecules, such as PP.

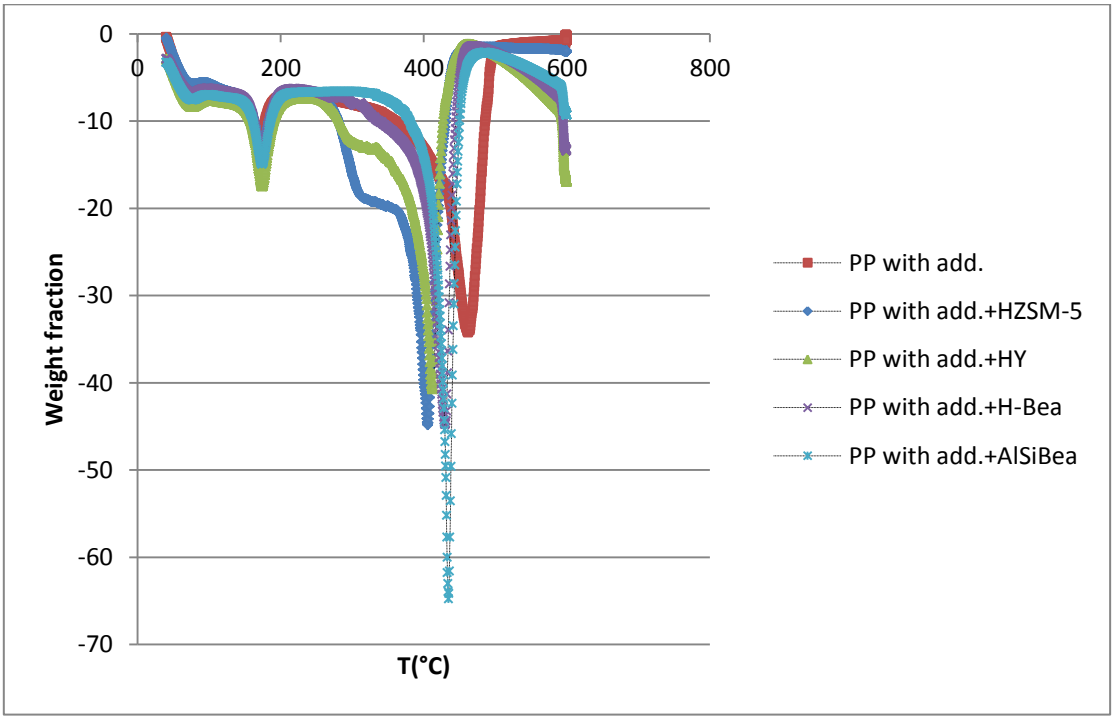

Figure 4. 8 – Heat Flow curves (DSC curves) obtained in the degradation of PP with additives for non-catalyzed and catalyzed process with different zeolites.

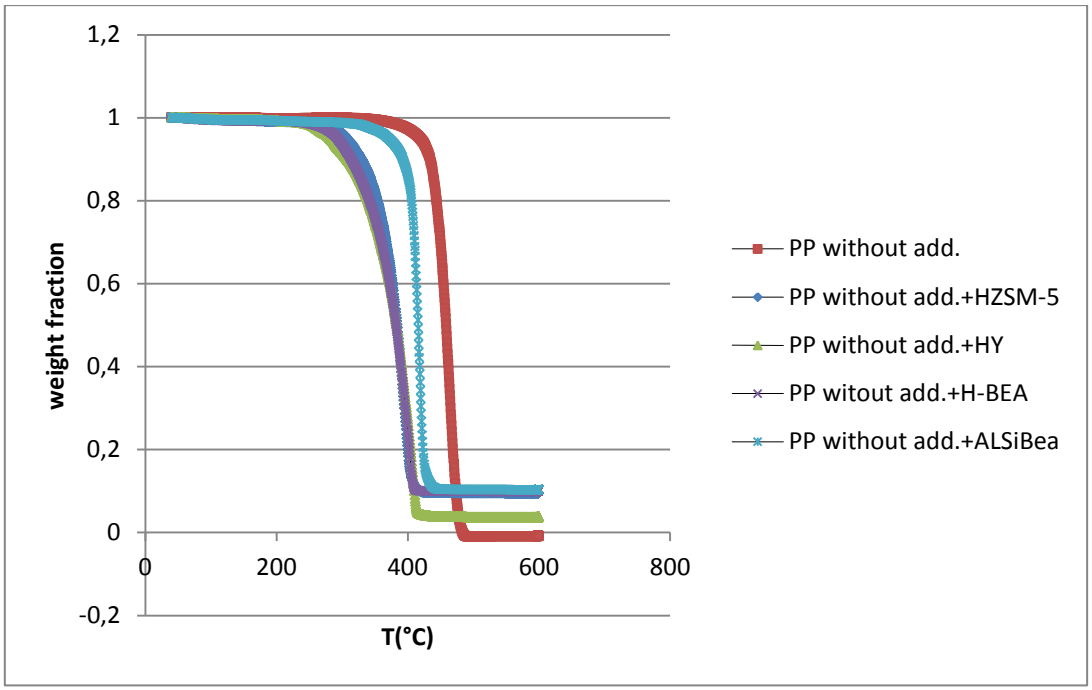

Figure 4. 9 – Weight loss curves (TGA curves) obtained in the degradation of PP without additives for non-catalyzed and catalyzed process with different zeolites.

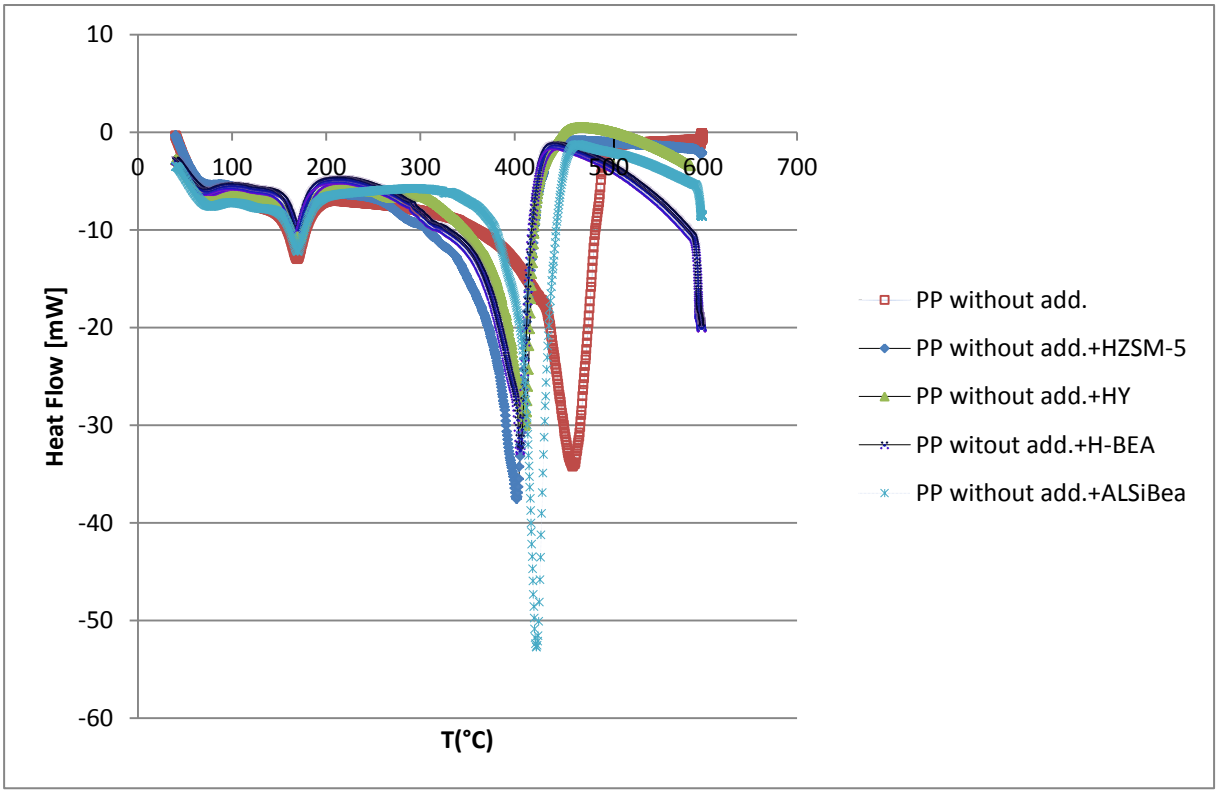

Figure 4. 10 - Heat Flow curves (DSC curves) obtained in the degradation of PP without additives for non-catalyzed and catalyzed process with different zeolites.

When we compare the different zeolites among each other, it can be seen (table 4.2) that the most effective catalyst for polymer degradation is HZSM-5. ZSM-5 has a high silicon to alumina ratio; the catalyst used in this set of experiments has ratio Si/Al=32 (see chapter 2). With proton (H^+) as the cation, the material becomes very acidic. Thus the acidity is proportional to the Al content. For both types of polypropylenes, the lowering of degradation temperature with the presence of HZSM-5 was approximately 50 °C.

The second best catalyst from the zeolites family was HY. The main properties of this catalyst are its high concentration of active acid sites, high thermal stability and high shape selectivity. With the Si/Al ratio equal 23 it can be predicted that HY is a good zeolite for the cracking reactions. Comparable with the HZSM-5, presence of HY also lowered the temperature of degradation for approximately 50 °C. This is observed for both types of polypropylene, with and without additives.

The presence of H-Bea catalyst lowered the temperature of degradation from 458 °C (thermal degradation) to 427 °C (polypropylene with additives) and 405 °C (polypropylene without additives). In this case there is a significant difference between lowering the degradation temperature with both types of polypropylenes. This catalyst is reported to have Brønsted acid sites in the micropores and on the external surface, and Lewis acid sites predominantly at the internal surface.

The last analysed catalyst from the zeolites, is the Bea type. In the table 4.2 it can be observed, that its presence during the degradation process of polypropylene with additives lowers the temperature degradation approximately 25 °C, and for the experiment with polypropylene without additives approximately 35 °C. It can be concluded that both zeolites, Bea and H-Bea have better influence for the degradation of polypropylene without additives (see table 4.2). As mentioned in chapter 1, zeolites are known for strong acidity and high specific surface area, but those characteristics are not enough for being excellent cracking catalysts. It was also suggested that initial polyolefin cracking occurs mainly at the acid sites on the external surface of a zeolite. Only small enough intermediates are able to enter the zeolite pores or channels and react with the internal acid sites of the zeolite. The external surface area plays more important role than the internal one for cracking of large molecules like polyolefin plastics to valuable small hydrocarbon molecules. Zeolite Bea has Si/Al ratio equal 150, which can be too high for this kind of process.

Table 4. 2 - Degradation temperature for PP with additives (a) and without additives (b) with catalysts: HZSM-5, HY, H-Bea, AlSiBea obtained from TGA/DSC results. Heating rate: 10°C/min.

Sample	$T_{degrad.}$(°C)
PP with additives	458,90
PP with add.+ HZSM-5	404,113
PP with add.+ HY	410,638
PP with add.+ H-Bea	427,034
PP with add.+ Bea	433,92

Sample	$T_{degrad.}$(°C)
PP without additives	459,00
PP with add.+ HZSM-5	400,912
PP with add.+ HY	408,30
PP with add.+ H-Bea	405,11
PP with add.+ Bea	422,04

4.3 Montmorillonites

4.3.1 DSC/TG analysis.

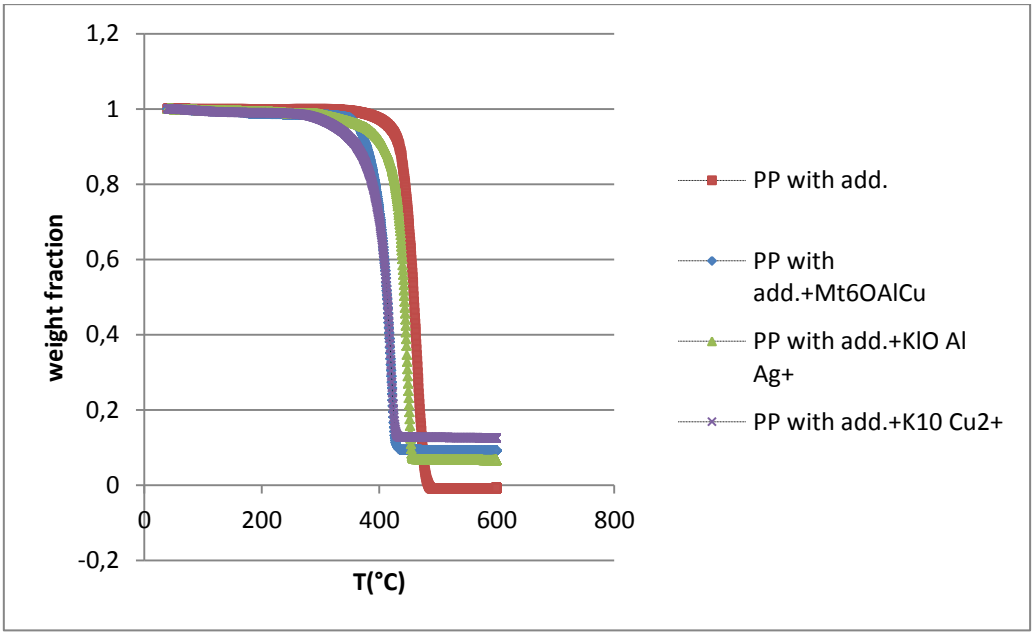

Figure 4. 11 - Weight loss curves (TGA curves) obtained in the degradation of PP with additives for non-catalyzed and catalyzed process with different montomorillonites.

In this subsection, results from the experiments with montmorillonites are shown. From this group of catalysts 3 representative samples were studied: Mt_6OAlCu, K10 Al Ag^+, K10 Cu^{2+}. The same methodology, discussed in the previous sections, was applied. A comparison of the activity of catalyst at a heating rate 10 °C/min in TGA/DSC experiments is shown in figures 4.11-4.14.

A very good catalytic effect was observed from the set of experiments with Mt_6OAlCu. As can be observed in figures 4.11 – 4.14 and table 4.3, this catalyst lowered the temperature of degradation from 458 °C to 412 °C (polypropylene with additives), and from 459 °C to 433 °C (polypropylene without additives).

The catalysts from the K10 montmorillonite series, K10 Al Ag^+ and K10 Cu^{2+}, also reduce the temperature of the degradation relatively to the non-catalytic process, although this reduction is a minor one, only about 10 – 20 °C.

All of the catalyst from the montmorillonite group were previously acidity – activated, what changed some properties of them. As mentioned in chapter 1, this activation extends the external surface area and alters the pore size distribution, which has a significant meaning for the cracking of hydrocarbons

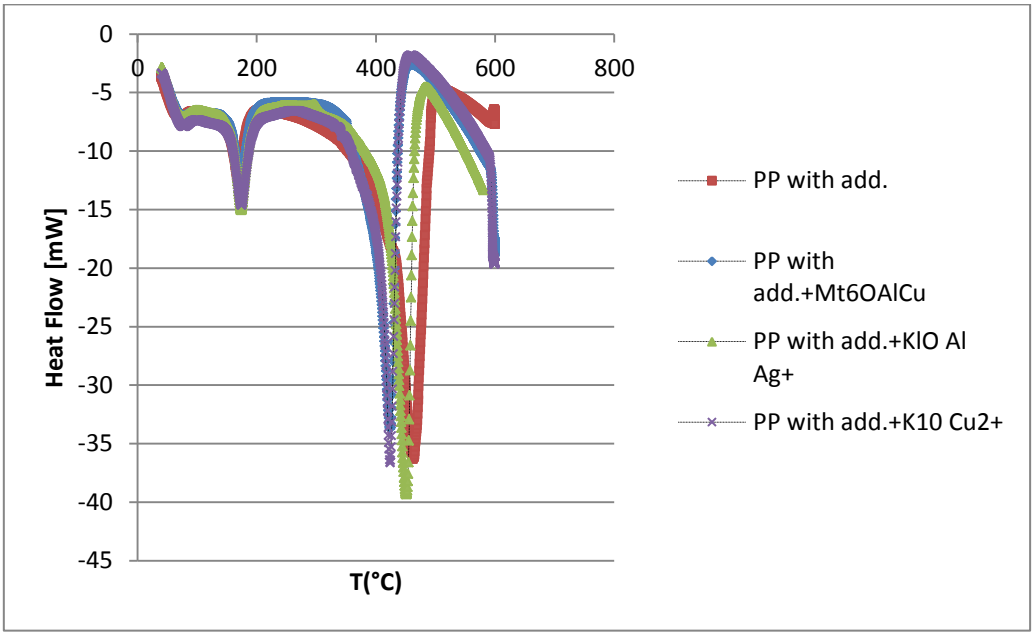

Figure 4. 12 – Heat Flow curves (DSC curves) obtained in the degradation of PP with additives for non-catalyzed and catalyzed process with different montomorillonites.

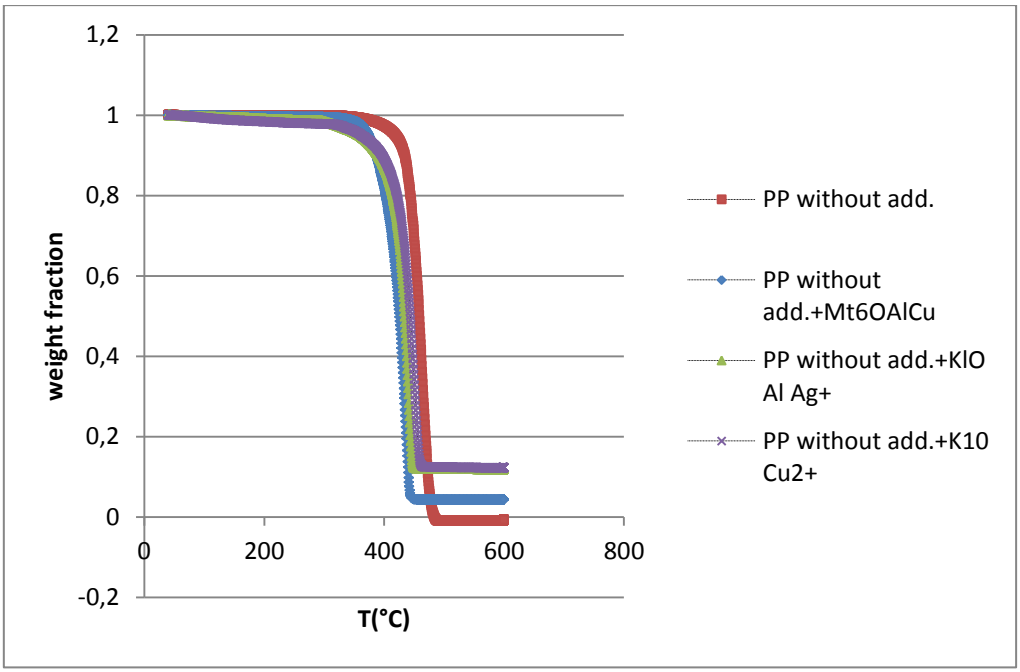

Figure 4. 13 - Weight loss curves (TGA curves) obtained in the degradation of PP without additives for non-catalyzed and catalyzed process with different montomorillonites.

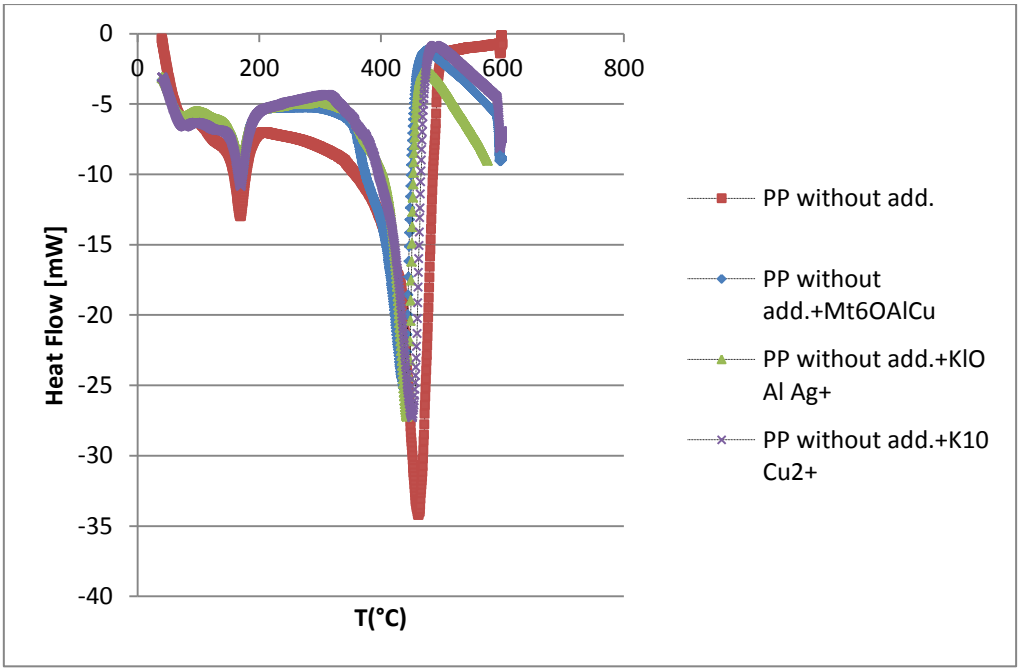

Figure 4. 14 – Heat Flow curves (DSC curves) obtained in the degradation of PP without additives for non-catalyzed and catalyzed process with different montomorillonites.

Table 4. 3 - Degradation temperature for PP with additives (a) and without additives (b) with catalysts: Mt_6OAlCu, K10 Al Ag^+, K10 Cu^{2+}, obtained from TGA/DSC results. Heating rate: 10°C/min.

Sample	$T_{degrad.}$(°C)
PP with additives	458,90
PP with add.+ Mt_6OAlCu	421,17
PP with add.+ K10 Al Ag^+	447,22
PP with add.+ K10 Cu^{2+}	422,19

Sample	$T_{degrad.}$(°C)
PP without additives	459,00
PP with add.+ Mt_6OAlCu^{2+}	433,18
PP with add.+ K10 Al Ag^+	440,39
PP with add.+ K10 Cu^{2+}	447,17

4.4. Deactivation Studies.

Additional subsection for the chapter with catalytic degradation of polypropylene, is the study of deactivation of two the best representatives from the tested catalysts, namely HY (zeolites) and Mt_6OAlCu (montmorillonites). To test the activity the procedure explained below were implemented.

Experiments were done on the polypropylene with additives samples under heating rate 10°C/min. Each experiment had 2 cycles: first one was the classic DSC/TG analysis; 2 mg of catalysts was added to the sample of polypropylene, and experiment were implemented (methodology description in chapter 2). After the first cycle of experiments a new portion of polypropylene were added to the catalyst used in previous cycle and the sequence is repeated. This we can check if the catalysts still retain the activity after use. This procedure was applied to both HY and Mt_6OAlCu catalysts.

4.4.1 DSC/TG analysis.

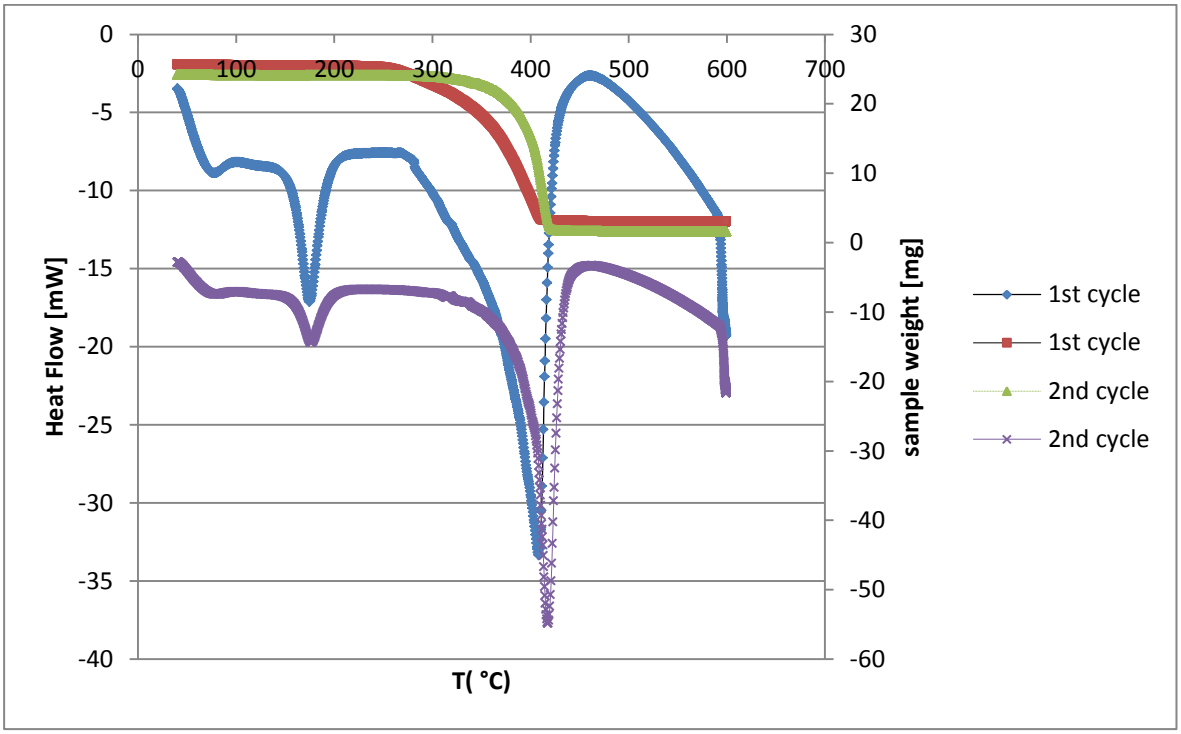

Figure 4. 15 - TGA and DSC curves obtained for the degradation of PP with additives, with presence of HY, for the 1st and 2nd cycle (heating rate 10°C/min).

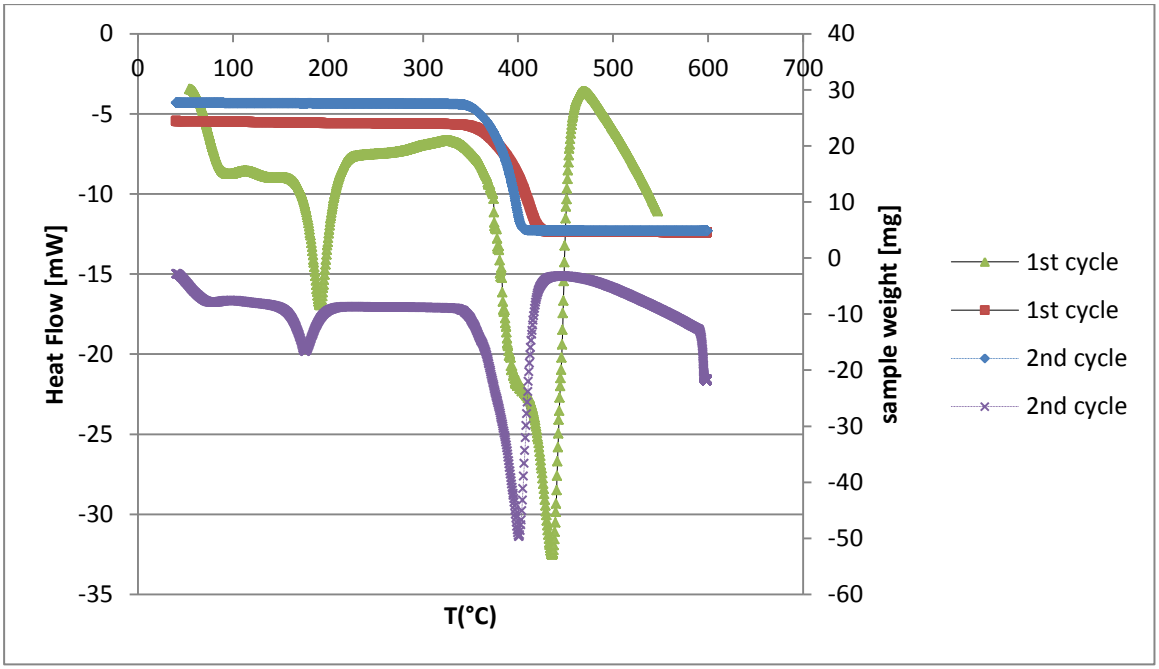

Figure 4. 16 - TGA and DSC curves obtained for the degradation of PP with additives, with presence of Mt_6OAlCu, for the 1st and 2nd cycle (heating rate 10°C/min).

As observed in the figure 4.15 and table 4.4, HY catalyst reduce the temperature degradation of polypropylene in both cycles: from 458 °C to 405 °C (first cycle), and to 416 °C (second cycle) This means that its activity decreased but, nevertheless, still maintains a significant activity. Possible explanation for this change in activity is that there might occur phenomena such as coking, which is usual during catalytic cracking reactions. It is a kind of catalyst deactivation due to coke formation on the catalyst surface. With occurrence of coke residues on the catalysts surface, total external surface is decreasing, as well as the number of acidic sites.

Unexpectedly, different results occurred for the experiments when use Mt_6OAlCu catalyst. As it can be seen in the table 4.4, this catalyst lowers the temperature degradation of polypropylene from 458 °C to 414 °C in the first cycle and to 400 °C in the second one. Improving in catalyst activity in second use is quite unusual. There is a possibility, that increasing temperature of experiment change somehow the properties of catalyst, improving it in case of cracking features. Likewise, there is a probability that products formed in the first cycle reacted with the catalyst, influencing its properties. Unfortunately, it cannot be uniquely identified, based only on the DSC/TGA analysis.

Table 4. 4 - Degradation temperature for PP with additives with HY (a) and Mt_6OAlCu (b), obtained from TGA/DSC results. Heating rate: 10°C/min.

Sample	**$T_{degrad.}$(°C)**
PP with additives	458,90
HY 1st cycle	405,20
HY 2nd cycle	416,00

Sample	**$T_{degrad.}$(°C)**
PP with additives	458,90
Mt_6OAlCu 1st cycle	414,323
Mt_6OAlCu 2nd cycle	400,123

CHAPTER 5. Final Conclusions

5.1 Achieved Results

The pyrolytic behavior of PP with and without additives samples has been studied using TGA/DSC apparatus, for thermal and catalytic degradation.

The conclusions drawn from this work are as follows:

The simultaneous use of DSC/TG analysis provided a clear picture of the thermal and catalytic degradation processes, allowing to have a look at the reaction that occurs within the polymer before gas-phase products start to evolve. This method provided additional information enabling better understanding of the plastic decomposition mechanism.

- Comparison between the thermal degradation of PP with and without additives (Dependence on type of polypropylene)
  Degradation temperature:

The degradation temperature of the pyrolysis process is dependent mostly on the heating rates. As observed, when heating rate increase, the maximum of the heat flow curves shift towards higher temperatures. Possible explanation is due to the kinetics of the process itself and to dynamic effects of the used equipment. This behavior occurs to both types of polypropylene.

Kinetic parameters

The computational model developed gives quite good fittings to the experimental values and allowed us to estimate kinetic and thermodynamic parameters in terms of the description of the chemical process involved. The estimated values for the bond energies, vaporization enthalpies and specific heat capacities are similar to published and calculated values.

In addition, in relation to apparent activation energy of the process determined for different heating rates and increase in the estimated activation energy as the heating rate increases was observed in accordance with the shift of the products distribution towards lighter ones.

- Comparison between the catalytic and thermal degradation
  Degradation temperature:

The catalytic pyrolysis of polypropylene with and without additives was also investigated using DSC/TGA analysis. For this study, although various catalysts were tested, zeolite catalysts were the most active catalysts on the reduction of the degradation temperature, with the best results for HZSM-5 and HY. Very good results were obtained for the Mt_6OAlCu from montmorillonites group. In contrast, vermiculites, both with transition metals and acidic activated, showed an apparent inactivity proving to be ineffective in the reduction of temperature process.

5.2 Future Trends

This work was a first approach to the study of thermal and catalytic degradation of polypropylene with and without additives.

Its development allowed to arrive at some important conclusions and opened perspectives for an additional research, with the goal of getting a better insight into the process. Likewise, some aspects of the pyrolysis that was not yet clarified, can be understand now more deeply.

In future work it may be interesting to extend the study to analyze waste polypropylene, as well as other types of polyolefins.

In case of catalyst degradation, although the zeolites turned out to be the best catalyst for pyrolysis, there are a lot of studies for its influence on plastics degradation. More promising will be testing catalysts belonging the montmorillonites, for comparative and more detailed analysis of the influence in the catalytic degradation of polyolefins. Consequently, a better characterization of the catalysts will be needed, namely in terms of surface area, acidity, pore structures and composition.

To develop a sustainable pyrolysis process, it will be required to have a detailed knowledge of the dependence between cracking conditions and product distributions.

Furthermore, evolution of the detailed kinetic measurements and computational models to explain the time-course evolution of the reaction as well as product distribution. Therefore, more detailed qualitative and quantitative characteristics of the products composition obtained in the degradation reaction is necessary.

Bibliography

[1] G. Scott; Polymers and environment, Royal Society of Chemistry (1999).

[2] William D. Callister; David G. Rethwish; Materials Science and Engineering, Eigth Edition

[3] Asociation of Plastics Manufacturers in Europe (APME); An Analysis of European Plastics Production, demand and waste data for 2011 (2012).

[4] C.L. Beyler and M. M. Hirschler; Thermal decomposition of polymers, In PJ Dinenno (ed), SFPE Hanbook of Fire Protection Engineering. 3rd edn, Quincy, Boston (2001).

[5] N_2 and CO_2 Adsorption by TMA- and HDP-Montmorillonites - C. Volzone*, J. O. Rinaldi, J. Ortiga Centro de Tecnología de Recursos Minerales y Cerámica (CETMIC)-CONICETC.C. 49, Cno. Centenario y 506, (1897) M. B. Gonnet, Prov. Buenos Aires, Argentina.

[6] Converting Plastic into a Resource; United Nations Environmental Programme Division of Technology, Industry and Economics International Environmental Technology Centre Osaka/Shiga, Japan; United Nations Environment Programme, 2009

[7] K. Laidler Chemical Kinetics; Second Edition

[8] H. Bockhorn, A. Hornung, U. Hornung; J. Anal. Appl. Pyrolysis, 50 (1999) 77.

[9] F. Torrens, G. Castellano; Int. J. Quantum Chem., 107 (2007) 2378.

[10] A. Corma; Chem. Rev. 95 (1995) 559.

[11] T. Butcko; Ph.D. Thesis, Institut fur Materialphysik, University at Wien (2004).

[12] M. Elanany, M. Koyama, M. Kubo, P. Selvan, A. Miyamoto; Microporous Mesoporous Mater., 71 (2004) 51.

[13] M. H. W. Sonoemans, C. den Heijer, and M. Crocker; J. Phys. Chem., 97 (1993) 440.

[14] M. Elanany, M. Koyama, M. Kubo, E. Broclawik, A. Miyamoto; Appl. Surf. Sci., 246 (2005)

[15] http://www.vermiculite.org/pdf_word/Vermiculite_Horticultural_Brochure.pdf

[16] M. Valáškov and G. Simha Martynková; Vermiculite: Structural Properties and Examples of the Use, Technical University of Ostrava,2012.

[17] L. Chmielarz, A. Kowalczyk, M. Michalik; Acid-activated vermiculites and phlogophites as catalysts for the DeNOx process; Applied Clay Science,2010

[18] B. Lombardi, M. Baschini, R.M. Torres Sanchez, Characterization of montmorillonites from bentonite deposits of North Patagonia, Argentina: Pchysicochemical and structural parameter correlation, 202

[19] J.F. Lambert, G. Poncelet; Top. Catal., 4 (1997) 43.

[20] J.M. Hartwell, The diverse uses of montmorillonites, 6,111.

[21] F.J. Mastral, E. Esperanza, P. Garcia, M. Just; Appl. Pyrolysis, 63 (2002) 273.

[22] J.M. Encinar, J.F. González; Fuel Process. Technol., 89 (2008) 678.

[23] R. W. J. Westerhout, J. Waanders, J. A. M. Kuipers, W. P. M. van Swaai; Ind. Eng. Chem. Res., 36 (1997) 1955.

[24] N. Kiran, E. Ekinci, C.E. Snape; Resour. Conserv. Recycl., 29 (2000) 273.

[25] J. Aguado, D.P. Serrano, G. San Miguel, M.C. Castro, S. Madrid; J. Anal. Appl. Pyrolysis, 79(2007) 415.
[26] A. Demirbas; J. Anal. Appl. Pyrolysis, 72 (2004) 97.
[27] L. Sorum, M. G. Gronl, J. E. Hustad; Fuel, 80 (2001) 1217.
[28] L. Ballice; Fuel, 80 (2001) 1923.
[29] H. Bockhorn, A. Hornung, U. Hornung; J. Anal. Appl. Pyrolysis, 50 (1999) 77.
[30] J. W. Park, S. Cheon Oh, H. P. Lee, H. T. Kim, K. OK Yo; Poly. Degrad. Stab., 67(2000)535.
[31] H. Bockhorn, A. Hornung, U.Hornung,P. Jakobstroer; J. Anal. Appl. Pyrolysis; 46 (1998) 1.
[32] S. Kim, E. Jang, D. Shin, K. Lee; Polym. Degrad. Stab., 85 (2004) 799.
[33] G. Manos, I.Y. Yusof, N. Papayannakos, N.H. Ganngas; Ind. Eng. Chem. Res., 40 (2001) 2220.
[34] I. Kayacan , Ö. M. Do Gan; Energy Sources, Part A, 30 (2008) 385.
[35] Z. Gao, I. Amasaki, M. Nakata; J. Anal. Appl. Pyrolysis, 67 (2003) 1.
[36] J. A. Conesa, A. Marcilla, R. Font, J.A. Caballero; J. Anal. Appl. Pyrolysis, 36 (1996) 1.
[37] G. Elordi, M. Olazar, R. Aguado, G. Lopez, M. Arabiourrutia and J. Bilbao; J. Anal. Appl. Pyrolysis, 79 (2007) 450.
[38] Q. Zhou, L. Zheng, Y.-Z. Wang. G.-M. Zhao, B. Wang; Polym. Degrad. Stab., 84 (2004) 493.
[39] Y.-H. Lin, M.-H. Yang; Appl. Catal. B, 69 (2007) 145.
[40] A. Garforth, S. Fiddy, Y.-H. Lin, A. Ghanbari-Siakhali, P.N. Sharratt; Thermochim. Acta, 294 (1997) 65.
[41] A. G. Buekens, H. Huang; Resour. Conserv. Recycl., 23 (1998), 163.
[42] Y. H. Lin, M.-H. Yang, T.-F.Yeh, M.-D. Ger; Polym. Degrad. Stab., 86 (2004) 121.
[43] K. Gobin, G. Manos; Polym. Degrad. Stab., 83 (2004) 267.
[44] K. Gobin, G. Manos; Polym. Degrad. Stab., 86 (2004) 225.
[45] A. Marcilla, J.A. Reyes-Labarta, F.J. Sempere; Polymer, 42 (2001) 5343.
[46] J.A. Reyes-Labarta, M.M. Olaya, A. Marcilla; Polymer, 47 (2006) 8194.
[47] S. Chaianansutcharit, R. Katsutath, A. Chaisuwan, T. Bhaskar, A. Nigo, A. Muto and Y. Sakata; J. Anal. Appl. Pyrolysis, 80 (2007) 360.
[48] A. Marcilla, A. Gómez-Siurana, F. Valdés; J. Anal. Appl. Pyrolysis, 79 (2007) 433.
[49] H. Bockhorn, A. Hornung, U. Hornung, D. Schawaller; J. Anal. Appl. Pyrolysis, 48 (1999) 93.
[50] F.J. Mastral, E. Esperanza, P. García, M. Juste; J. Anal. Appl. Pyrolysis, 63 (2002) 1.
[51] J.M. Encinar, J.F. González; Fuel Process. Technol., 89 (2008) 678.
[52] R. W. J. Westerhout, J. Waanders, J. A. M. Kuipers, W. P. M. van Swaai; Ind. Eng. Chem. Res., 36 (1997) 1955.
[53] N. Kiran, E. Ekinci, C.E. Snape; Resour. Conserv. Recycl., 29 (2000) 273.
[54] J. Aguado, D.P. Serrano, G. San Miguel, M.C. Castro, S. Madrid; J. Anal. Appl. Pyrolysis, 79 (2007) 415.
[55] R. W. J. Westerhout, J. Waanders, J. A. M. Kuipers, W. P. M. van Swaai; Ind. Eng. Chem. Res., 36 (1997) 1955.
[56] J. Ceamanos, J.F. Mastral, A. Millera, M.E. Aldea; J. Anal. Appl. Pyrolysis, 65 (2002) 93.
[57] J. W. Park, S. Cheon Oh, H. P. Lee, H. T. Kim, K. OK Yo; Poly. Degrad. Stab., 67(2000).

[58] http://commons.wikimedia.org/wiki/File:Syndiotactic-polypropylene-3D-balls.png

[59] R. Ramos Pinto, P. Borges, M.A.N.D.A. Lemos, F. Lemos, J.C. Védrine, E.G. Derouane, F. Ramôa Ribeiro, Appl. Catal. A 284 (2005) 39–46

[60] 10th International Chemical and Biological Engineering Conference,CHEMPOR 2008- '*Thermal degradation kinetics of polyethylene in dynamic conditions using simultaneous DSC/TG analysis'* A. Coelho, L. Costa, M.M. Marques, I.M. Fonseca, M.A.N.D.A. Lemos, F. Lemos.

[61] '*Thermal degradation kinetics of polyethylene in dynamic conditions using simultaneous DSC/TG analysis'* A. Coelho, L. Costa, M.M. Marques, I.M. Fonseca, M.A.N.D.A. Lemos, F. Lemos, unpublished work.

APPENDIX A. DATA ANALYSIS

Table A.1.1 – Experimental runs done in this work.

Sample	Total initial mass(mg)	Finall mass (mg)	Tdegrad.(°C)	Initial mass polymer (mg)	Mass of catalyst (mg)	Heating rate (°C /min)
PP with add. 10°C/min	**17,95**	**0,39**	**458,95**	**17,95**	**0**	**10**
PP with add.20°C/min	**21,03**	**0,27**	**477,17**	**21,03**	**0**	**20**
PP with add. 40°C/min	**37,32**	**0,44**	**488,17**	**37,32**	**0**	**40**
PP without add.10°C/min	**17,28**	**-0,16**	**459,01**	**17,28**	**0**	**10**
PP without add.20°C/min	**11,26**	**0,12**	**472,93**	**11,26**	**0**	**20**
PP without add.40°C/min	**14,5**	**0,03**	**494,67**	**14,5**	**0**	**40**
PP with add.+HZSM-5	**19,57**	**3,16**	**404,11**	**16,41**	**3,16**	**10**
PP without add.+HZSM-5	**18,41**	**1,71**	**400,91**	**16,69**	**1,72**	**10**
PP with add.+HY	**24,07**	**1,65**	**410,64**	**1,44**	**22,62**	**10**
PP without add+HY	**17,33**	**0,67**	**408,3**	**15,35**	**1,98**	**10**

PP with add.+H-Bea	**18,14**	**0,87**	**427,04**	**17,26**	**0,884**	**10**
PP without add.+H-Bea	**14,83**	**1,49**	**405,11**	**13,31**	**1,52**	**10**
PP with add.+Bea	**18,32**	**1,38**	**433,92**	**16,46**	**1,86**	**10**
PP without add.+Bea	**16,86**	**1,89**	**422,03**	**15,32**	**1,54**	**10**
PP with add.+Mt6OAlCu	**17,21**	**1,56**	**422,19**	**15,65**	**1,32**	**10**
PP without add.+Mt6OAlCu	**14,84**	**0,65**	**433,19**	**13,17**	**1,47**	**10**
PP with add.+ K10AlAg	**20,58**	**1,38**	**447,22**	**18,97**	**1,61**	**10**
PP without add.+K10AlAg	**13,98**	**1,65**	**440,39**	**11,9**	**2,08**	**10**
PP with add.+K10Cu	**21,36**	**2,64**	**422,19**	**17,74**	**3,62**	**10**
PP without add.+K10Cu	**17,26**	**2,08**	**447,76**	**15,57**	**1,69**	**10**
PP with add.+VERZrAg	**16,48**	**3,38**	**453,76**	**14,59**	**1,89**	**10**
PP without add.+VerZrAg	**16,27**	**3,56**	**456,36**	**12,39**	**3,88**	**10**
PP with add.+VerZrCu	**18,72**	**2,26**	**455,86**	**14,77**	**4,1**	**10**

PP without add.+VerZrCu	**15,3**	**1,62**	**453,88**	**12,9**	**2,4**	**10**
PP with add.+VerAlAg	**22,04**	**2,05**	**455,87**	**19,02**	**3,02**	**10**
PP without add.+VerAlAg	**16,35**	**2,24**	**456,95**	**14,921**	**1,44**	**10**
PP with add.+VerAlCu	**19,7**	**2,05**	**454,87**	**17,69**	**2,01**	**10**
PP without add.+VerAlCu	**18,57**	**2,6**	**456,09**	**16,13**	**2,44**	**10**
PP with add.+VH Ag	**18,58**	**2,47**	**455,87**	**16,88**	**1,7**	**10**
PP without add.+VH Ag	**17,05**	**0,72**	**456,3**	**16,52**	**0,53**	**10**
PP with add.+ VH Cu	**19,09**	**0,99**	**459,03**	**18,1**	**0,99**	**10**
PP without add.+Vh Cu	**17,1**	**1,4**	**458,04**	**16,08**	**1,02**	**10**